



TECHNICAL UNIVERSITY OF CRETE

**OPTIMAL DESIGN AND ENERGY
MANAGEMENT IN RES-H₂ HYBRID
SYSTEMS**

By

Loukidou Elissavet

A thesis submitted to the Department of Production Engineering and Management

Technical University of Crete

In fulfillment of the Requirements for the diploma of

Production Engineering and Management

Chania, September 2023

Supervisor: **Dimitrios Ipsakis**, Assistant Professor

Abstract

The purpose of this thesis is to develop an operational algorithm for designing a system that aims to optimize the utilization of energy generated by photovoltaic panels while ensuring system autonomy. Excess energy is used to produce a specific quantity of hydrogen (water electrolysis) by the end of each year.

In the first chapter, the thesis emphasizes the need to move away from conventional energy production methods relying on fossil fuels due to the serious issues they cause, including limited energy resources and environmental pollution from greenhouse gas emissions. Consequently, the thesis proposes hydrogen as an alternative energy source to address these problems.

The second chapter presents the mathematical models of the subsystems used, including the photovoltaic system, the Lead-Acid battery, the electrolysis unit, and the hydrogen storage system.

The third chapter explains the energy management algorithm, which considers the State Of Charge (SOC) of the battery as a control variable to determine the operating conditions of all system components for optimal performance. To protect the accumulator from frequent start-stop cycles, a hysteresis band is introduced into the algorithm, making operational limits more flexible.

Finally, in the fourth chapter, the use of the Optimization Tool package in Matlab, employing genetic algorithms, is explained. This optimization aims to determine the optimal sizes of the subsystems (photovoltaic system, accumulator, and electrolysis unit) that will lead to a predetermined H₂ production by the end of each year. Based on this algorithm and the meteorological data in the areas of Anogia and Tavronitis, various scenarios are examined for meeting the energy needs of specific communities (with one or without any house), while simultaneously achieving a specific goal of hydrogen production. Some results were obtained in this regard:

- In the area of Anogia, the production of 2000000 liters of hydrogen is achieved by using photovoltaic systems. For community 1, a photovoltaic system with a capacity of 6.9 kW is employed, while for community 2, a photovoltaic system with a capacity of 43.7 kW is utilized. To meet the energy requirements of community 1, batteries with a capacity of 844.2 Ah are used, whereas for community 2, batteries with a capacity of 30344.2 Ah are employed. Additionally, an electrolysis unit with a size of 8.4 kW is used for community 1, while for community 2, an electrolysis unit with a size of 8.5 kW is employed. In order to offset the expenses of the above equipment over a 20-year period, with the aim of achieving a net present value of zero, it was calculated that the

produced hydrogen should be sold at 16.8€ for community 1 and 60.8€ for community 2.

- In the area of Tavronitis, the production of 2000000 liters of hydrogen is achieved by using photovoltaic systems. For community 1, a photovoltaic system with a capacity of 8.8 kW is employed, while for community 2, a photovoltaic system with a capacity of 55.1 kW is utilized. To meet the energy requirements of community 1, batteries with a capacity of 1740.6 Ah are used, whereas for community 2, batteries with a capacity of 25240.6 Ah are employed. Additionally, an electrolysis unit with a size of 9.1 kW is used for community 1, while for community 2, an electrolysis unit with a size of 9.2 kW is employed. In order to offset the expenses of the above equipment over a 20-year period, with the aim of achieving a net present value of zero, it was calculated that the produced hydrogen should be sold at 20.3€ for community 1 and 81.4€ for community 2.
- In the area of Anogia, the production of 20000000 liters of hydrogen is achieved by using photovoltaic systems. For community 1, a photovoltaic system with a capacity of 70.8 kW is employed, while for community 2, a photovoltaic system with a capacity of 153.8 kW is utilized. To meet the energy requirements of community 1, batteries with a capacity of 6865.5 Ah are used, whereas for community 2, batteries with a capacity of 6865.5 Ah are employed. Additionally, an electrolysis unit with a size of 51.9 kW is used for community 1, while for community 2, an electrolysis unit with a size of 51.9 kW is employed. In order to offset the expenses of the above equipment over a 20-year period, with the aim of achieving a net present value of zero, it was calculated that the produced hydrogen should be sold at 15.3€ for community 1 and 22.8€ for community 2.
- In the area of Tavronitis, the production of 20000000 liters of hydrogen is achieved by using photovoltaic systems. For community 1, a photovoltaic system with a capacity of 84.5 kW is employed, while for community 2, a photovoltaic system with a capacity of 132.4 kW is utilized. To meet the energy requirements of community 1, batteries with a capacity of 21487.1 Ah are used, whereas for community 2, batteries with a capacity of 21487 Ah are employed. Additionally, an electrolysis unit with a size of 129.8 kW is used for community 1, while for

community 2, an electrolysis unit with a size of 129.8 kW is employed. In order to offset the expenses of the above equipment over a 20-year period, with the aim of achieving a net present value of zero, it was calculated that the produced hydrogen should be sold at 21.6€ for community 1 and 27.8€ for community 2.

- In the area of Anogia, the production of 200000000 liters of hydrogen is achieved by using photovoltaic systems. For community 1, a photovoltaic system with a capacity of 638.8 kW is employed, while for community 2, a photovoltaic system with a capacity of 698.8 kW is utilized. To meet the energy requirements of community 1, batteries with a capacity of 119660.6 Ah are used, whereas for community 2, batteries with a capacity of 119660.6 Ah are employed. Additionally, an electrolysis unit with a size of 838.7 kW is used for community 1, while for community 2, an electrolysis unit with a size of 838.7 kW is employed. In order to offset the expenses of the above equipment over a 20-year period, with the aim of achieving a net present value of zero, it was calculated that the produced hydrogen should be sold at 15.9€ for community 1 and 16.7€ for community 2.
- In the area of Tavronitis, the production of 200000000 liters of hydrogen is achieved by using photovoltaic systems. For community 1, a photovoltaic system with a capacity of 837.2 kW is employed, while for community 2, a photovoltaic system with a capacity of 897.2 kW is utilized. To meet the energy requirements of community 1, batteries with a capacity of 89208.1 Ah are used, whereas for community 2, batteries with a capacity of 89208.1 Ah are employed. Additionally, an electrolysis unit with a size of 586.5 kW is used for community 1, while for community 2, an electrolysis unit with a size of 586.5 kW is employed. In order to offset the expenses of the above equipment over a 20-year period, with the aim of achieving a net present value of zero, it was calculated that the produced hydrogen should be sold at 17.7€ for community 1 and 16.7€ for community 2.

Key words: hydrogen, renewable energy sources (RES), solar energy, greenhouse gases, energy problem, environmental problem, water electrolysis, energy management algorithm.

Περίληψη

Ο σκοπός της παρούσας διπλωματικής εργασίας είναι η δημιουργία ενός αλγορίθμου λειτουργίας για το σχεδιασμό ενός συστήματος που στοχεύει στη βέλτιστη αξιοποίηση της παραγόμενης ενέργειας από τα φωτοβολταϊκά πάνελ, εξασφαλίζοντας αυτονομία στο σύστημα. Η πλεονάζουσα ενέργεια χρησιμοποιείται για την παραγωγή συγκεκριμένης ποσότητας υδρογόνου (με ηλεκτρόλυση νερού) για την επίτευξη συγκεκριμένου στόχου στο τέλος κάθε χρόνου.

Στο πρώτο κεφάλαιο η διπλωματική εργασία τονίζει την αναγκαιότητα απομάκρυνσης από τις συμβατικές μεθόδους παραγωγής ενέργειας που βασίζονται στα ορυκτά καύσιμα λόγω των σοβαρών προβλημάτων που προκαλούν. Στα προβλήματα αυτά περιλαμβάνονται οι περιορισμένοι ενεργειακοί πόροι και η περιβαλλοντική ρύπανση που προκαλείται από τις εκπομπές αερίων του θερμοκηπίου. Έτσι, η διπλωματική εργασία προτείνει την υιοθέτηση του υδρογόνου ως εναλλακτική πηγή ενέργειας για την αντιμετώπιση αυτών των προβλημάτων.

Στο δεύτερο κεφάλαιο παρουσιάζονται τα μαθηματικά μοντέλα των υποσυστημάτων που χρησιμοποιήθηκαν, δηλαδή του φωτοβολταϊκού συστήματος, του συσσωρευτή Μολύβδου-Οξέος (μπαταρία), της μονάδας ηλεκτρόλυσης και του συστήματος αποθήκευσης του υδρογόνου.

Στο τρίτο κεφάλαιο εξηγείται ο αλγόριθμος διαχείρισης της ενέργειας, ο οποίος λαμβάνει υπόψη την κατάσταση φόρτισης (State Of Charge - SOC) της μπαταρίας ως μεταβλητή ελέγχου και καθορίζει τις συνθήκες λειτουργίας όλων των εξαρτημάτων του συστήματος, ώστε να εξασφαλίζεται η βέλτιστη απόδοσή τους. Για αυτόν το λόγο εισάγεται στον αλγόριθμο ένα φάσμα υστέρησης (Hysteresis band) το οποίο στοχεύει στη δημιουργία πιο ευέλικτων ορίων λειτουργίας για τον συσσωρευτή, με σκοπό την προστασία του από τη διακοπτόμενη χρήση που δρα αρνητικά στη διάρκεια ζωής του.

Τέλος, στο τέταρτο κεφάλαιο παρουσιάζεται ο τρόπος χρήσης του πακέτου βελτιστοποίησης, Optimization Tool, στο Matlab, χρησιμοποιώντας γενετικούς αλγορίθμους. Η βελτιστοποίηση αυτή στοχεύει στον προσδιορισμό των βέλτιστων μεγεθών των υποσυστημάτων (φωτοβολταϊκό σύστημα, μπαταρία και μονάδα ηλεκτρόλυσης) που οδηγούν σε μια προκαθορισμένη παραγωγή H₂ στο τέλος κάθε έτους. Με βάση τον αλγόριθμο αυτό και τα μετεωρολογικά δεδομένα για την περιοχή των Ανωγείων και την περιοχή του Ταυρωνίτη εξετάζονται διάφορα σενάρια για την κάλυψη των ενεργειακών αναγκών συγκεκριμένων κοινοτήτων (με ένα ή κανένα σπίτι), ενώ ταυτόχρονα επιτυγχάνεται και συγκεκριμένος στόχος παραγωγής H₂. Τα αποτελέσματα είναι τα εξής:

- Στην περιοχή των Ανωγείων, η παραγωγή 2000000 λίτρων υδρογόνου επιτυγχάνεται με χρήση φωτοβολταϊκών συστημάτων. Για την κοινότητα 1, χρησιμοποιείται ένα φωτοβολταϊκό σύστημα με χωρητικότητα 6.9 kW, ενώ για την κοινότητα 2 χρησιμοποιείται ένα φωτοβολταϊκό σύστημα με χωρητικότητα 43.7 kW. Για να καλυφθούν οι ενεργειακές ανάγκες της κοινότητας 1, χρησιμοποιούνται μπαταρίες με χωρητικότητα 844.2 Ah, ενώ για την κοινότητα 2 χρησιμοποιούνται μπαταρίες με χωρητικότητα 30344.2 Ah. Επιπλέον, χρησιμοποιείται μονάδα ηλεκτρόλυσης με μέγεθος 8.4 kW για την κοινότητα 1, ενώ για την κοινότητα 2 χρησιμοποιείται μονάδα ηλεκτρόλυσης με μέγεθος 8.5 kW. Για να μπορέσουν να μηδενιστούν τα έξοδα από την αγορά του παραπάνω εξοπλισμού σε διάστημα 20 χρόνων, δηλαδή η καθαρή παρούσα αξία να είναι μηδενική, υπολογίστηκε πως το παραγόμενο υδρογόνο θα πρέπει στην περίπτωση της κοινότητας 1 να πουληθεί 16.8€ και στην περίπτωση της κοινότητας 2 να πουληθεί 60.8€.
- Στην περιοχή του Ταυρωνίτη, η παραγωγή 2000000 λίτρων υδρογόνου επιτυγχάνεται με χρήση φωτοβολταϊκών συστημάτων. Για την κοινότητα 1, χρησιμοποιείται ένα φωτοβολταϊκό σύστημα με χωρητικότητα 8.8 kW, ενώ για την κοινότητα 2 χρησιμοποιείται ένα φωτοβολταϊκό σύστημα με χωρητικότητα 55.1 kW. Για να καλυφθούν οι ενεργειακές ανάγκες της κοινότητας 1, χρησιμοποιούνται μπαταρίες με χωρητικότητα 1740.6 Ah, ενώ για την κοινότητα 2 χρησιμοποιούνται μπαταρίες με χωρητικότητα 25240.6 Ah. Επιπλέον, χρησιμοποιείται μονάδα ηλεκτρόλυσης με μέγεθος 9.1 kW για την κοινότητα 1, ενώ για την κοινότητα 2 χρησιμοποιείται μονάδα ηλεκτρόλυσης με μέγεθος 9.2 kW. Για να μπορέσουν να μηδενιστούν τα έξοδα από την αγορά του παραπάνω εξοπλισμού σε διάστημα 20 χρόνων, δηλαδή η καθαρή παρούσα αξία να είναι μηδενική, υπολογίστηκε πως το παραγόμενο υδρογόνο θα πρέπει στην περίπτωση της κοινότητας 1 να πουληθεί 20.3€ και στην περίπτωση της κοινότητας 2 να πουληθεί 81.4€.
- Στην περιοχή των Ανωγείων, η παραγωγή 20000000 λίτρων υδρογόνου επιτυγχάνεται με χρήση φωτοβολταϊκών συστημάτων. Για την κοινότητα 1, χρησιμοποιείται ένα φωτοβολταϊκό σύστημα με χωρητικότητα 70.8 kW, ενώ για την κοινότητα 2 χρησιμοποιείται ένα φωτοβολταϊκό σύστημα με χωρητικότητα 153.8 kW. Για να καλυφθούν οι ενεργειακές ανάγκες της κοινότητας 1, χρησιμοποιούνται μπαταρίες με χωρητικότητα 6865.5 Ah, ενώ για την

κοινότητα 2 χρησιμοποιούνται μπαταρίες με χωρητικότητα 6865.5 Ah. Επιπλέον, χρησιμοποιείται μονάδα ηλεκτρόλυσης με μέγεθος 51.9 kW για την κοινότητα 1, ενώ για την κοινότητα 2 χρησιμοποιείται μονάδα ηλεκτρόλυσης με μέγεθος 51.9 kW. Για να μπορέσουν να μηδενιστούν τα έξοδα από την αγορά του παραπάνω εξοπλισμού σε διάστημα 20 χρόνων, δηλαδή η καθαρή παρούσα αξία να είναι μηδενική, υπολογίστηκε πως το παραγόμενο υδρογόνο θα πρέπει στην περίπτωση της κοινότητας 1 να πουληθεί 15.3€ και στην περίπτωση της κοινότητας 2 να πουληθεί 22.8€.

- Στην περιοχή του Ταυρωνίτη, η παραγωγή 20000000 λίτρων υδρογόνου επιτυγχάνεται με χρήση φωτοβολταϊκών συστημάτων. Για την κοινότητα 1, χρησιμοποιείται ένα φωτοβολταϊκό σύστημα με χωρητικότητα 84.5 kW, ενώ για την κοινότητα 2 χρησιμοποιείται ένα φωτοβολταϊκό σύστημα με χωρητικότητα 132.4 kW. Για να καλυφθούν οι ενεργειακές ανάγκες της κοινότητας 1, χρησιμοποιούνται μπαταρίες με χωρητικότητα 21487.1 Ah, ενώ για την κοινότητα 2 χρησιμοποιούνται μπαταρίες με χωρητικότητα 21487 Ah. Επιπλέον, χρησιμοποιείται μονάδα ηλεκτρόλυσης με μέγεθος 129.8 kW για την κοινότητα 1, ενώ για την κοινότητα 2 χρησιμοποιείται μονάδα ηλεκτρόλυσης με μέγεθος 129.8 kW. Για να μπορέσουν να μηδενιστούν τα έξοδα από την αγορά του παραπάνω εξοπλισμού σε διάστημα 20 χρόνων, δηλαδή η καθαρή παρούσα αξία να είναι μηδενική, υπολογίστηκε πως το παραγόμενο υδρογόνο θα πρέπει στην περίπτωση της κοινότητας 1 να πουληθεί 21.6€ και στην περίπτωση της κοινότητας 2 να πουληθεί 27.8€.
- Στην περιοχή των Ανωγείων, η παραγωγή 200000000 λίτρων υδρογόνου επιτυγχάνεται με χρήση φωτοβολταϊκών συστημάτων. Για την κοινότητα 1, χρησιμοποιείται ένα φωτοβολταϊκό σύστημα με χωρητικότητα 638.8 kW, ενώ για την κοινότητα 2 χρησιμοποιείται ένα φωτοβολταϊκό σύστημα με χωρητικότητα 698.8 kW. Για να καλυφθούν οι ενεργειακές ανάγκες της κοινότητας 1, χρησιμοποιούνται μπαταρίες με χωρητικότητα 119660.6 Ah, ενώ για την κοινότητα 2 χρησιμοποιούνται μπαταρίες με χωρητικότητα 119660.6 Ah. Επιπλέον, χρησιμοποιείται μονάδα ηλεκτρόλυσης με μέγεθος 838.7 kW για την κοινότητα 1, ενώ για την κοινότητα 2 χρησιμοποιείται μονάδα ηλεκτρόλυσης με μέγεθος 838.7 kW. Για να μπορέσουν να μηδενιστούν τα έξοδα από την αγορά του παραπάνω εξοπλισμού σε διάστημα 20 χρόνων, δηλαδή η καθαρή παρούσα αξία να είναι μηδενική, υπολογίστηκε πως το παραγόμενο υδρογόνο θα πρέπει

στην περίπτωση της κοινότητας 1 να πουληθεί 15.9€ και στην περίπτωση της κοινότητας 2 να πουληθεί 16.7€.

- Στην περιοχή του Ταυρωνίτη, η παραγωγή 200000000 λίτρων υδρογόνου επιτυγχάνεται με τη χρήση φωτοβολταϊκών συστημάτων. Για την κοινότητα 1, χρησιμοποιείται ένα φωτοβολταϊκό σύστημα με χωρητικότητα 837.2 kW, ενώ για την κοινότητα 2 χρησιμοποιείται ένα φωτοβολταϊκό σύστημα με χωρητικότητα 897.2 kW. Για να καλυφθούν οι ενεργειακές ανάγκες της κοινότητας 1, χρησιμοποιούνται μπαταρίες με χωρητικότητα 89208.1 Ah, ενώ για την κοινότητα 2, χρησιμοποιούνται μπαταρίες με χωρητικότητα 89208.1 Ah. Επιπλέον, χρησιμοποιείται μονάδα ηλεκτρόλυσης με μέγεθος 586.5 kW για την κοινότητα 1, ενώ για την κοινότητα 2, χρησιμοποιείται μονάδα ηλεκτρόλυσης με μέγεθος 586.5 kW. Για να μπορέσουν να μηδενιστούν τα έξοδα από την αγορά του παραπάνω εξοπλισμού σε διάστημα 20 χρόνων, δηλαδή η καθαρή παρούσα αξία να είναι μηδενική, υπολογίστηκε πως το παραγόμενο υδρογόνο θα πρέπει στην περίπτωση της κοινότητας 1 να πουληθεί 17.7€ και στην περίπτωση της κοινότητας 2 να πουληθεί 16.7€.

Λέξεις κλειδιά: υδρογόνο, ανανεώσιμες πηγές ενέργειας (ΑΠΕ), ηλιακή ενέργεια, αέρια του θερμοκηπίου, ενεργειακό πρόβλημα, ηλεκτρόλυση νερού, αλγόριθμος διαχείρισης ενέργειας

Table of contents

Abstract	1
Περίληψη	4
Chapter 1: Energy and environmental concerns.....	9
1.1 Increased energy consumption and environmental impact	9
1.2 Hydrogen: The environmentally friendly energy carrier for a sustainable energy future.....	10
1.3 Hydrogen production through solar energy	11
Chapter 2: Mathematical modelling of the RES-H ₂ system	12
2.1 Photovoltaic system (PV System).....	12
2.2 Lead-Acid Accumulator.....	16
2.3 Electrolysis unit.....	20
2.4 Hydrogen storage system	23
Chapter 3: Energy control strategy	25
3.1 Description of energy control strategies.....	25
Chapter 4: Application and results of the energy control strategy.....	29
4.1 Scenarios for covering the energy needs of Community 1.....	33
4.2 Scenarios for covering the energy needs of Community 2.....	34
4.3 Recording of results for the energy needs coverage scenarios of community 1.....	35
4.3.1 Use of data from the area of Anogia.....	36
4.3.2 Use of data from the area of Tavroniti	40
4.4 Recording of results for the energy needs coverage scenario of community 2	45
4.4.1 Use of data from the area of Anogia.....	46
4.4.2 Use of data from the area of Tavroniti	50
Chapter 5: Conclusions and Future Steps	55
Literature.....	60
English	60
Greek.....	61

Chapter 1: Energy and environmental concerns

1.1 Increased energy consumption and environmental impact

Technological developments in recent years have led to a continuous increase in energy needs and demands. The global demand and production of energy are steadily increasing due to the large augmentation of the population combined with the industrial expansion in many countries and the uncontrolled use of energy. In 1990 the worldwide annual electricity consumption was approximately 110000TWh, while in 2022 the energy consumption reached almost 170000TWh, as illustrated in the following figure.

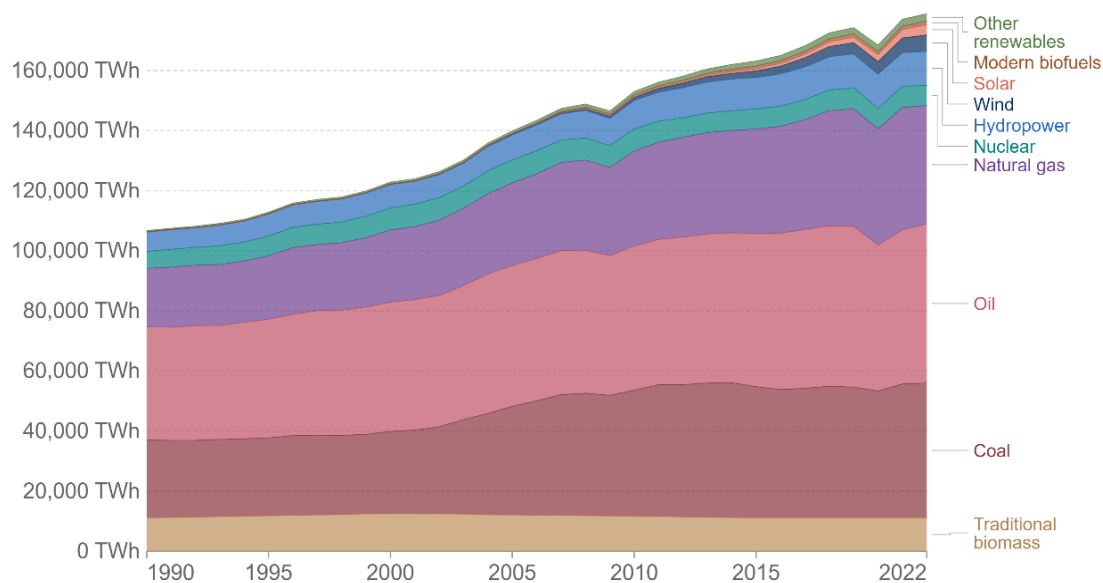


Figure 1.1 Global energy consumption from 1990 until 2022. **Source:** [1]

The available energy resources in our environment are divided into three main categories: fossil fuels (such as oil, gas, and coal), nuclear energy, and renewable energy sources. Most of the produced energy comes from fossil fuels, each with its own unique characteristics and origin.

The process of extracting fossil fuels has proven to be highly damaging. The combustion of hydrocarbons and coal-based fuels, which are used for electricity generation, releases significant amounts of CO₂ and other harmful substances into the atmosphere. This has led to irreversible damage to our environment and poses a significant risk of climate change due to the emissions of carbon dioxide (CO₂) from

fossil fuels. This threat is considered the main concern for both the environment and human health. Fossil fuels are not a viable option for the future as they are non-renewable energy sources. Their extensive use has caused irreparable harm to our planet. However, it is crucial to strike a balance between limiting their use with meeting human needs. The total global CO₂ emissions from 1990 to 2021 are shown below.

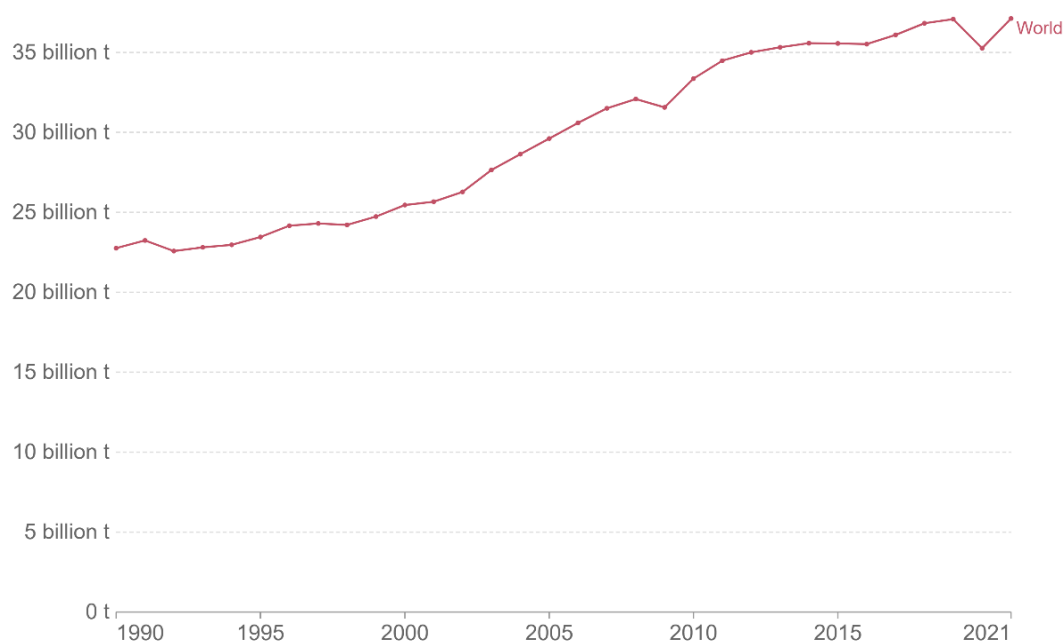


Figure 1.2 Total global CO₂ emissions from 1990 until 2021. **Source:** [1]

1.2 Hydrogen: The environmentally friendly energy carrier for a sustainable energy future

Renewable energy sources, such as solar, wind, hydro, geothermal, biomass, ocean currents, tides, and waves, have gradually become part of our energy production. These sources can be used for both electricity and fuel generation. Consequently, there is a growing need for the further integration of alternative energy sources that can serve not only as fuels, but also for electricity generation.

The solution to this challenge includes synthetic petrol, synthetic natural gas (methane), methanol, ethanol, and hydrogen. Among these alternatives, hydrogen has been chosen as a replacement for fossil fuels.

Hydrogen is considered an “eco-friendly” energy carrier because it does not release carbon byproducts when used in fuel cells or internal combustion engines. It is also highly suitable for transportation, easily convertible into other forms of energy, and exhibits high energy efficiency. Moreover, hydrogen is economically viable, safe to

use, and environmentally compatible. It can be employed as a substitute for fossil fuels in industrial processes, contributing to ammonia production and innovative forms of methanol production. Moreover, hydrogen serves as an efficient means to transport renewable energy over long distances and enables the storage of large amounts of energy. Additionally, it finds utility as a vehicle fuel, particularly for long-distance transportation and heavy-duty vehicles such as trucks, ships, and airplanes, due to its higher energy density compared to batteries.

1.3 Hydrogen production through solar energy

In solar energy technologies, sunlight is used to produce heat and electricity. Direct solar energy, also known as solar photovoltaic power, refers to a system that converts solar radiation into electrical energy through photovoltaic cells. Solar power, and particularly photovoltaic systems, can offer a viable alternative solution. Compared to other renewable energy sources, it provides the most stable and predictable energy supply while offering cost-effective installation units.

Hydrogen can be produced from renewable energy sources through the process of water electrolysis without emitting carbon dioxide and without using fossil fuels. This method uses electricity to separate hydrogen from oxygen in water. In a typical hydrogen photovoltaic system, a photovoltaic generator supplies electricity to a water-electrolyzer.

The system is illustrated in Figure 1.3. To store large quantities, hydrogen can be stored either underground or in aquifers and subsequently transported through pipelines to energy consumption centers.

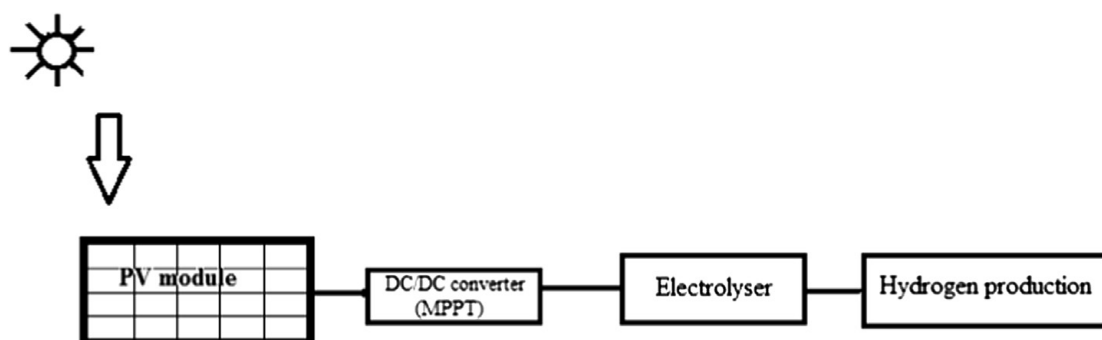


Figure 1.3 A typical photovoltaic hydrogen system. Source: [2]

Chapter 2: Mathematical modelling of the RES-H₂ system

The material used in chapter 2 and 3 is sourced from the thesis of Ipsakis Dimitris, titled "Design of optimal operation of energy systems using renewable and alternative sources", completed in 2011 as a PhD thesis at Aristotle University of Thessaloniki.

This chapter presents the theoretical background for the operation of each subsystem. It will describe the main aspects of the mathematical equations used in the Matlab environment for the simulation of the system. These equations aim to model the fundamental characteristics of the subsystems employed.

The subsystems used and analyzed below are:

- Photovoltaic system (PV Arrays)
- Lead-Acid Accumulator
- Electrolysis unit
- Hydrogen storage system

2.1 Photovoltaic system (PV System)

A photovoltaic system consists of the photovoltaic panels, the supporting installation of these panels, and the auxiliary equipment, mainly comprises of electrical parts. The core component of the panel is the silicon solar cell, where several elements are connected in series in order to increase both the delivered voltage and the power output.

Photovoltaic panels are composed of two types of semiconductors, a positive "p" (p-type) and a negative "n" (n-type). At room temperature, n-type semiconductors contain numerous freely moving electrons, while p-type semiconductors contain many freely moving positive charges, known as electron holes. The interface between the two semiconductors forms a p-n junction, which functions as a diode.

If the diode is exposed to photons of solar radiation with energy levels higher than the band gap (e_{gap}) of the semiconductor, then the number of free electrons in the "p" semiconductor and the number of positive charges in the "n" semiconductor increase and an electric field is created. Consequently, the electrons at the p-pole move and reach the diode region, where they are attracted by the positive field of this region. By connecting the semiconductors in an external circuit, we have the creation of an electric current.

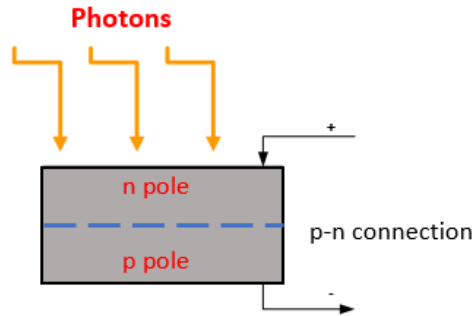


Figure 2.1 Operating principle of a solar cell. **Source:** [7]

Photons with energy above a specific threshold have the ability to initiate this effect. The magnitude of the generated current depends on the element's surface area and the concentration of active photons in solar radiation. During the night, the photovoltaic panel is considered inactive device, producing neither current nor voltage. However, if it remains connected to an external source, the diode I_D current (or dark current) is generated.

The positioning of the panels in relation to the sun depends on the geographical location of the installation area (altitude, hemisphere, etc.), and typically, the optimal installation angle is provided by information from space exploration agencies, such as NASA.

The mathematical analysis of photovoltaic system operation is based on the characteristic current-voltage (I-V) curve, which depends on the intensity of solar radiation and the air temperature at the surface of the photovoltaic cell. The equivalent circuit that can describe the proposed model is presented below and serves as the foundation for the development of various mathematical models of photovoltaic systems found in established literature.

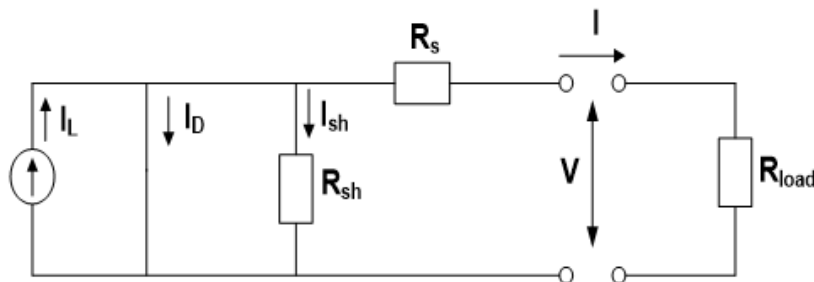


Figure 2.2 Equivalent electrical operating circuit of a photovoltaic cell. **Source:** [7]

According to Kirchoff's current law applies to the above circuit:

$$I = I_L - I_D - I_{sh} \tag{2.1}$$

where:

I: the operating current, A

I_L: the photodiode current, A

I_D: the diode current, A

I_{sh}: the deflection current, A

From the semi-empirical analysis of the currents in relation (2.1), the relation power → incident radiation + temperature is exhibiting a strongly non-linear behavior. This relationship gives the connection between the intensity I (A) and the operating voltage V_{PV} (Volt) for the above circuit:

$$I = I_{pv} = I_L - I_D - I_{sh} = I_L - I_O \cdot \left[\exp\left(\frac{V_{pv} + I_{pv} \cdot R_s}{\alpha}\right) - 1 \right] - \frac{V_{pv} + I_{pv} \cdot R_s}{R_{sh}} \quad (2.2)$$

where:

- R_s: the resistance in series, V
- R_{sh}: the shunt resistance, V
- α: the correlation parameter for curve fitting, V
- I_D: the reverse diode saturation current, A
- V_{pv}: the operating voltage of the element, V

Considering high the difference between the two resistances, R_{sh} >> R_s, the above equation is further simplified by removing the last term as follows:

$$I_{pv} = I_L - I_O \cdot \left[\exp\left(\frac{V_{pv} + I_{pv} \cdot R_s}{\alpha}\right) - 1 \right] \quad (2.3)$$

In order to solve (2.3), equations that take into account extreme operating conditions. Such conditions are required. Such conditions involve the current and voltage values under short-circuit, open-circuit, and maximum power conditions, as described below.

At short circuit conditions with zero V_{pv}, the current I_L flowing through the diode is equal to the short circuit current. It can be expressed as:

$$I_{L,ref} = I_{PV,sc,ref} = I_{PV} = I_{sc,ref} \quad (2.4)$$

The term ref indicates the reference conditions:

- Solar radiation G_{ref} = 1000 W/m²
- Air temperature T_{ref} = 25 °C

At open circuit conditions with zero current $I_{pv} = 0$, the unit is dropped from equation (2.3) because it is a very small term compared to the exponential term, so equation (2.3) is transformed to:

$$I_{o,oc,ref} = I_{L,ref} \cdot \exp\left(\frac{-V_{oc,ref}}{\alpha_{ref}}\right) \quad (2.5)$$

If the values of intensity I_{pv} and voltage V_{pv} are substituted at maximum power conditions, i.e. $I_{pv}=I_{mp,ref}$ and $V_{pv}=V_{mp,ref}$ and substituting (2.4) and (2.5) into (2.3), the relationship for the series resistance can be derived as:

$$R_{s,ref} = \frac{\alpha_{ref} \cdot \ln\left(1 - \frac{I_{mp,ref}}{I_{L,ref}}\right) - V_{mp,ref} + V_{oc,ref}}{I_{mp,ref}} \quad (2.6)$$

In addition, the effect of solar radiation and temperature on the term α , I_L , and I_o mentioned in the basic equation (2.3) is introduced as follows:

$$\alpha = \alpha_{ref} \frac{T_c}{T_{c,ref}} \quad (2.7)$$

$$I_L = \frac{G_T}{G_{T,ref}} \cdot [I_{L,ref} + \mu_{I,sc} \cdot (T_c - T_{c,ref})] \quad (2.8)$$

$$I_o = I_{o,ref} \left(\frac{T_c}{T_{c,ref}}\right)^3 \cdot \exp\left[\left(\frac{e_{gap} \cdot N_s}{\alpha_{ref}}\right) \cdot \left(1 - \frac{T_c}{T_{c,ref}}\right)\right] \quad (2.9)$$

$$e_{gap} = 1.17 - 4.73 \cdot 10^{-4} \cdot \frac{T_c^2}{T_c + 636} \quad (2.10)$$

where:

- T_c : the temperature of the element, K
- G_T : solar radiation, W/m²
- N_s : the number of solar cells in the photovoltaic panel
- e_{gap} : the dead bandwidth of the construction material, eV
- $T_{c,ref}$: the reference temperature, 25 °C
- $G_{T,ref}$: reference solar radiation, 1000 W/m²

By modifying relation (2.5) in terms of temperature and using relations (2.5), (2.7), and (2.9) can be obtained the determination of the parameter α_{ref} , which is required to complete the mathematical description of the photovoltaic system:

$$\alpha_{ref} = \frac{\mu_{V,oc} \cdot T_{c,ref} - V_{oc,ref} + e_{gap} \cdot N_s}{\frac{\mu_{I,sc} \cdot T_{c,ref}}{I_{L,ref}} - 3} \quad (2.11)$$

Relations (2.3) - (2.11) essentially form the set of equations describing the operation of a photovoltaic panel. The power dissipated by the PV array is given as:

$$P_{pv} = V_{pv} \cdot I_{pv} \cdot n_{pv} \cdot N_{panel} \quad (2.12)$$

where:

- P_{pv} : the power produced by the photovoltaic system, W
- N_{panel} : the number of photovoltaic panels
- n_{pv} : the efficiency of the system

The system efficiency, n_{pv} , includes all electrical losses during power generation and usually corresponds to a value close to ~90%.

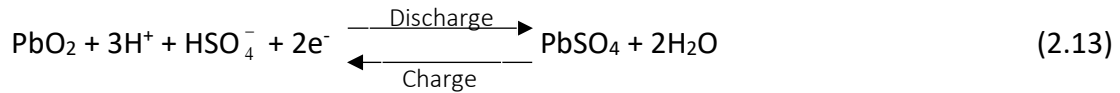
2.2 Lead-Acid Accumulator

An autonomous power generation system, designed to account the fluctuating nature of solar energy, requires the installation of short-term energy storage. This storage system not only temporarily stores excess energy from renewable sources but also serves as a means to supply immediate power to meet part of the demand load during energy shortage periods. However, the primary focus of the system's operating algorithm is to protect the storage device, known as the accumulator, from potential overcharging and complete discharge, aiming to prolong its lifespan.

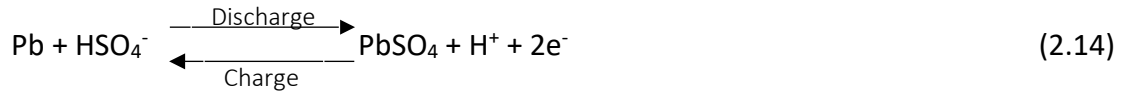
Accumulators, commonly known as batteries, are widely used for energy storage and conversion. They convert stored chemical energy into electrical energy (and reverse) through a series of electrochemical reactions. The basic functional unit of accumulators is the electrochemical cell, which is connected in series and parallel to increase voltage and capacity, respectively. During discharge, oxidation occurs at the anode (negative electrode), releasing electrons into an external circuit, while reduction takes place at the cathode (positive electrode), utilizing the generated electrons. Lead-acid batteries, specifically, employ chemical reactions involving lead dioxide (PbO₂) as the cathode electrode, lead (Pb) as the anode electrode, and sulfuric acid (H₂SO₄) as the electrolyte, facilitating the flow of electric current between the anode and the cathode through ions. The separator, a porous

membrane, allows the movement of ions between the electrodes. The chemical processes occurring in a lead-acid "cell" are described by the following reactions:

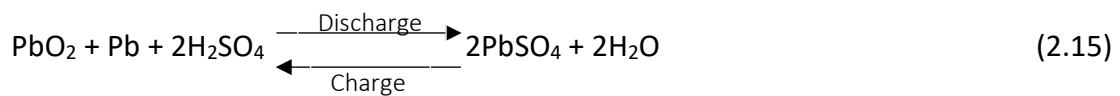
Cathode (positive electrode)



Anode (negative electrode)



Total Reaction (double sulfate reaction)



During discharge, both lead dioxide and lead undergo a conversion process and are transformed into lead sulfate (PbSO₄).

The accumulator, functioning as an electrical system, is regarded as a voltage source that is connected in series with a resistor, as illustrated below:

$$V_{ac} = E_{ac} - I_{ac} \cdot R_o \quad (2.16)$$

$$P_{ac} = V_{ac} \cdot I_{ac} \quad (2.17)$$

where:

- E_{ac}: the internal voltage, V
- R_o: the internal resistance, Ω
- V_{ac}: the operating voltage, V
- I_{ac}: the operating current, A
- P_{ac}: the power (charging and discharging), W

Figure 2.3 simulates the basic operation of the accumulator using a comparable configuration of two communicating containers connected through a valve (conductivity) permitting the flow of liquid between the two containers. Container A1 (the same symbol also indicates its volume) represents the load that is directly available for use, while container A2 symbolizes the load stored chemically in the accumulator.

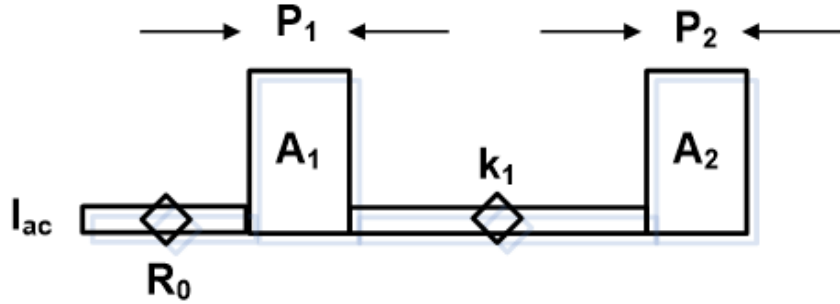


Figure 2.3 Lead-acid accumulator kinetic simulation model. **Source:** [7]

The conductivity k_1 (proportional to the difference between P_1 and P_2), corresponds to the rate constant of a first-order chemical reaction that expresses the process where the bound charge becomes available. Each of the two containers is

characterized by an amplitude determined by the term P_i where, according to the literature [3], applies:

- $P_1 > P_2$
- $P_2 = 1 - P_1 = 1 - c$.

The sum of the volumes of containers A_1 and A_2 essentially correspond to the maximum possible utilization of the nominal capacity of the accumulator (q_{\max}) in Ah.

The dynamic equations in Figure 2.3, which relate the charges (in Ah) q_1 (available) and q_2 (bound) to the heights, h_i , of containers A_1 and A_2 are given as follows:

$$\frac{dq_1}{dt} = -I_{ac} - k_1 \cdot (h_1 - h_2) \quad (2.18)$$

$$\frac{dq_2}{dt} = k_1 \cdot (h_1 - h_2) \quad (2.19)$$

$$h_1 = \frac{A_1}{P_1} = \frac{q_1}{c} \quad (2.20)$$

$$h_2 = \frac{A_2}{P_2} = \frac{q_2}{1-c} \quad (2.21)$$

where:

- k_1 : conductivity, S
- c : the width of each tank, m
- q_1 : the available charge (available charge), Ah
- q_2 : the bound charge, Ah

- I_{ac} : the intensity of the charging or discharging current, A
- h_1, h_2 : the height of containers 1 and 2 respectively, m
- t : the operating time, h

In the above set of equations, if relations (2.20) and (2.21) are substituted into (2.18) and (2.19), it follows that the loads q_1 and q_2 are given as:

$$q_1 = q_{1,0} \cdot e^{-k \cdot t} + \frac{(q_0 \cdot k \cdot c - I_{ac}) \cdot (1 - e^{-k \cdot t})}{k} - \frac{I_{ac} \cdot c \cdot (k \cdot t - 1 + e^{-k \cdot t})}{k} \quad (2.22)$$

$$q_2 = q_{2,0} \cdot e^{-k \cdot t} + q_0 \cdot (1 - c) \cdot (1 - e^{-k \cdot t}) - \frac{I_{ac} \cdot (1 - c) \cdot (k \cdot t - 1 + e^{-k \cdot t})}{k} \quad (2.23)$$

$$k = \frac{k_1}{c \cdot (1 - c)} \quad (2.24)$$

where:

- $q_{1,0}, q_{2,0}$: the initial available and committed load respectively, Ah
- q_0 : the sum of the loads $q_{1,0}$ and $q_{2,0}$, $q_0 = q_{1,0} + q_{2,0}$, Ah
- k, c : parameters calculated for each accumulator from manufacturing data

The maximum discharge and charge currents can be determined by setting the left-hand side of equation (2.22) equal to ($q_1=0$) and ($q_1=c \cdot q_{max}$) after a certain time t . These currents are given by the following equations:

$$I_{d,max} = \frac{k \cdot q_{1,0} \cdot e^{-k \cdot t} + q_0 \cdot k \cdot c \cdot (1 - e^{-k \cdot t})}{1 - e^{-k \cdot t} + c \cdot (k \cdot t - 1 + e^{-k \cdot t})} \quad (2.25)$$

$$I_{c,max} = \frac{-k \cdot c \cdot q_{max} + k \cdot q_{1,0} \cdot e^{-k \cdot t} + q_0 \cdot k \cdot c \cdot (1 - e^{-k \cdot t})}{1 - e^{-k \cdot t} + c \cdot (k \cdot t - 1 + e^{-k \cdot t})} \quad (2.26)$$

where:

- $I_{d,max}$: the maximum discharge current for time t , A
- $I_{c,max}$: the maximum charging current for time t , A

As shown in relation (2.16), the voltage of the accumulator is a linear function of resistance, internal voltage, and current. The operating temperature is assumed to be constant.

The value of the internal voltage, E_{ac} , is obtained from the following relations for the case of discharge and charge:

Discharge

$$E_{ac} = E_{\min} + (E_{o,d} - E_{\min}) \cdot \frac{q_1}{q_{1,\max}} \quad (2.27)$$

Charge

$$E_{ac} = E_{o,c} + (E_{\max} - E_{o,c}) \cdot \frac{q_1}{q_{1,\max}} \quad (2.28)$$

where:

- E_{\min} : the minimum required internal discharge voltage, V
- $E_{o,d}$: the maximum acceptable internal discharge voltage, V
- E_{\max} : the maximum required internal charging voltage, V
- $E_{o,c}$: the minimum acceptable internal charging voltage, V

The above values of internal voltages are provided from manufacturing data, which are widely accessible and refer to the extreme operating conditions of the battery during full discharge and charge.

The main variable of the operation of the batteries and, more generally, of the integrated renewable energy sources (RES) utilization module, is the state of charge (SOC). It is the control variable that indicates the capacity of the accumulator in percentage terms and is related to the charge/discharge current and the available stored charge at any given time. Although the state of charge (SOC) cannot be directly measured, it can be obtained through other measurements, such as voltage, or through mainly empirical methods that require highly complex techniques. Essentially, SOC represents the ratio of the available load at time t to the nominal capacity of the accumulator and is given, according to the existing literature, [6], as:

$$SOC(t+1) = SOC(t) \cdot (1 - \sigma_{ac}) + \frac{I_{ac} \cdot \eta_{ac}}{Q_o} \cdot (\Delta t) \quad (2.29)$$

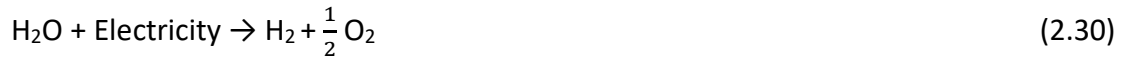
where:

- η_{ac} : the performance of the accumulator ~95%
- σ_{ac} : the self-discharge rate of the accumulator ~2.5%
- Δt : the difference of the time moments $(t+1)-t$, h

2.3 Electrolysis unit

The electrolysis system consists of tanks that generate pure hydrogen and oxygen. This process utilizes electrical energy to decompose water into hydrogen and oxygen. Similar to accumulators, electrolysis tanks consist of electrochemical cells

with anode and cathode electrodes, as well as an electrolyte that aids in the transportation of ions. At the cathode, protons are reduced to form hydrogen, while at the anode, water undergoes oxidation to produce oxygen and protons, releasing two electrons in the process. As a result, hydrogen accumulates at the cathode, while oxygen concentrates at the anode. In summary, the overall reaction can be described as follows:



The simulation employs a PEM (Polymer Electrolyte Membrane) type electrolysis tank, which ensures high-purity H₂ and exhibits excellent performance at high current density levels. In PEM electrolysis tanks, a combination of materials such as iridium, ruthenium, platinum, and graphite is used for the anode, while platinum or platinum-graphite is utilized for the cathode. The PEM electrolysis, illustrated in Figure 2.4, is characterized by the use of a polymeric fluorocarbon ionomer membrane, specifically of the Nafion[®] type, which selectively permits only the passage of protons. These protons are hydrogen ions (H⁺), which are separated from water and oxygen when they pass through the membrane, forming hydrogen molecules (H₂). The advantages of this setup include the elimination of a liquid electrolyte that requires continuous recirculation and its high potential for integration into renewable energy recovery systems with intermittent energy production. Consequently, the PEM electrolysis device offers significant benefits and is appropriately proposed for implementation in the integrated plant under investigation.

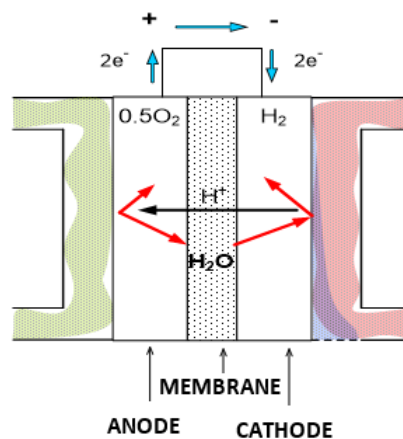


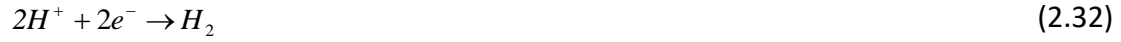
Figure 2.4 Operation of an electrochemical cell during the electrolysis process using polymeric membrane. **Source:** [7]

The electrochemical reactions of the electrolysis device are presented below followed by a description of their operation for each case.

Anode



Cathode



The fundamental equation describing how the electrolysis device corresponds to the voltage-current (V-I) relationship. This relationship takes into account the losses resulting from electrostatic interactions and resistances during the transfer of electrons and ions.

The V-I relationship for an electrochemical cell and the necessary electrical power are given as follows:

$$P_{elec} = V_{elec} \cdot I_{elec} \cdot n_{elec} \quad (2.33)$$

$$V_{elec} = V_{rev,elec} + \frac{r_1 + r_2 \cdot T_{elec}}{A_{elec}} \cdot I_{elec} + (s_1 + s_2 \cdot T_{elec} + s_3 \cdot T_{elec}^2) \cdot \log\left(\frac{t_1 + t_2/T_{elec} + t_3/T_{elec}^2}{A_{elec}} \cdot I_{elec}\right) \quad (2.34)$$

where:

- V_{elec} : the operating voltage of the cell, V
- I_{elec} : the operating current of the electrolysis device, A
- P_{elec} : the consumed power of the electrolysis device, W
- n_{elec} : number of cells of the electrolysis device
- r_1 and r_2 : parameters related to electrolyte resistance, $\Omega \cdot m^2$ and $\Omega \cdot m^2 / ^\circ C$ corresponding
- s_1 , s_2 and s_3 : parameters related to the losses in the electrodes, V, $V / ^\circ C$ and $V / ^\circ C^2$ corresponding
- t_1 , t_2 και t_3 : parameters related to the losses in the electrodes, $V \cdot m^2 / A$, $V \cdot m^2 \cdot ^\circ C / A$ and $V \cdot m^2 \cdot ^\circ C^2 / A$ corresponding
- A_{elec} : the surface of the electrodes, m^2
- T_{elec} : the operating temperature of the electrolysis device, $^\circ C$

The rate at which hydrogen is produced in an electrolysis tank, comprising multiple cells connected in series, is directly related to the electrical input and is given by Faraday's law:

$$n_{H_2} = n_F \cdot \frac{n_c \cdot I_{elec}}{n_e \cdot F} \quad (2.35)$$

where:

- n_{H_2} : the rate of hydrogen production, mol/s
- n_c : the number of cells of the electrolysis apparatus in series
- n_F : the Faraday efficiency
- F : Faraday constant, 96485 As mol⁻¹
- n : number of electrons per water molecule

The Faraday efficiency is defined as the ratio between the actual and theoretical maximum hydrogen production and is mainly given by manufacturing companies at values of 80-100%.

2.4 Hydrogen storage system

Hydrogen storage can be accomplished either in liquid or gaseous form, utilizing a two-stage process. Initially, the hydrogen produced by the electrolyzer is stored in a small temporary storage tank until a predetermined pressure ($P_{buffer,max}$) is reached. This tank is called a buffer. When the buffer is full, the hydrogen is transferred to the compressor, where it undergoes simultaneous pressure increase and is transferred to the final storage tanks. In these tanks, the hydrogen is first compressed and then transferred to the central tank for storage. The transfer and compression of the hydrogen last until the pressure in the buffer reaches the value of $P_{buffer,min}$. This approach primarily ensures optimal operation of the compressor by protecting it from continuous use and effectively smoothes out the intermittent hydrogen production, which occurs with different flows each time.

The operational storage scheme proposed for an integrated RES utilization unit is presented in Figure 2.5 and is distinguished by the implementation of short-term storage units.

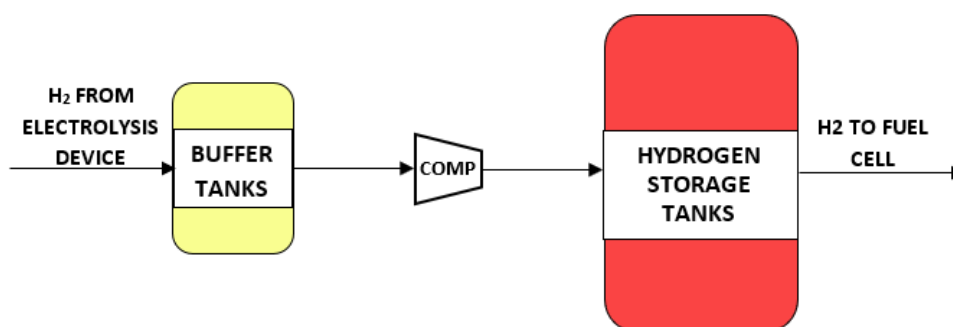


Figure 2.5 Functional principle of hydrogen storage in an integrated RES utilization unit / Schematic illustration of H₂ storage connectivity. **Source:** [7]

The fundamental mathematical model describing the pressure in both the buffer and the central tank involves the Van der Waals law equation for real gases. This model relates the storage pressure, the volume of the containers, the storage temperature (which remains practically constant), and the hydrogen inflow:

$$P_T = \frac{n \cdot R \cdot T_{stor}}{V_T - n \cdot b} - a \cdot \frac{n^2}{V_T^2} \quad (2.36)$$

$$a = \frac{27 \cdot R^2 \cdot T_{cr}^2}{64 \cdot P_{cr}} \quad (2.37)$$

$$b = \frac{R \cdot T_{cr}}{8 \cdot P_{cr}} \quad (2.38)$$

where:

- P_T: the storage pressure, bar
- n: the number of linear molecules of stored hydrogen, mol
- R: the global gas constant, bar·m³/mol·K
- T_{stor}: the storage temperature of hydrogen, K
- V_T: the volume of the storage tank, m³
- T_{cr} και P_{cr}: the critical temperature and pressure of hydrogen respectively, K and bar
- α: the term to describe the intermolecular actions, bar·m⁶/mol²
- β: the term describing the volume occupied by the gas molecules of a mole, m³/mol.

However, in the present thesis, the buffer storage will not be used, but is presented here for completeness.

Chapter 3: Energy control strategy

This chapter will present the energy control strategy, which uses the energy produced by the photovoltaic to meet the demand load. In case of excess energy, it can either charge the accumulator or be converted into hydrogen through water electrolysis and stored. In situations of energy deficit, the load is supported by supplying power from the accumulator. The steps used in this strategy include:

- Simulation of a photovoltaic system
- Identification of two cases based on the net power's sign
- Utilization of a control variable, the state of charge (SOC) of the accumulator, which determines hydrogen production and the interruption point
- Implementation of a hysteresis band to reduce strain on the subsystem

3.1 Description of energy control strategies

The fundamental principle guiding the simultaneous design and energy control strategy for the studied unit is to optimize the utilization of the energy generated by the photovoltaic panels to produce a defined quantity of H₂ by the end of the year, such as X kg/yr or Nm³/yr. However, to achieve this objective, optimal utilization of the connected subsystems is also necessary (e.g., accumulator SOC, charging/discharging cycles). The system's power at any given time is determined by the difference between the power generated by the PV panels, P_{res} (W), and the constant demand P_{load} (W), which can refer to one or more houses.

$$P = P_{res} - P_{load} \quad (2.39)$$

Consequently, the resulting power determines whether we have a deficit ($P < 0$) or excess power ($P > 0$), depending on its sign. Depending on whether the net power is positive or negative, we can identify two cases that enable the initiation of specific unit functions

If the net power is positive ($P > 0$):

- Battery charging/ discharging
- Operation of the electrolysis device
- Power rejection

If the net power is negative ($P < 0$):

- Battery discharging

However, in addition to the value of the net power, the operation of each subsystem also depends on the value of a control variable. The strategy developed for managing the generated power is based on the idea that the accumulator is responsible for smoothing out the energy fluctuations resulting from the photovoltaic panels, as its dynamics are much faster compared to the electrolyzer. Thus, the primary variable chosen to determine the operating conditions of the integrated photovoltaic panel utilization unit is the state of charge, SOC, of the accumulator. Decisions regarding specific operations will be made based on predefined limits for the accumulator's operation. In particular, the upper limit of the accumulator's operation, SOC_{max} , is proposed to determine hydrogen production, while the lower limit, SOC_{min} , is set to stop hydrogen production. At the same time, several technical specifications are presented to ensure the safe operation of the unit. One of the main objectives in the development of the control strategy is to consider all factors that impact the integrated unit's operation. Neglecting these details can lead to system malfunctions and consequently to extremely unfavorable costs.

The necessary steps for control strategy development before implementation in a RES process include:

- Compliance with the manufacturing operating limits for the accumulator and the electrolysis device.
- Determining the electrolysis device starting point by the excess net power and the maximum operating limit of the accumulator.
- Setting minimum power limits for the electrolysis device, as well as a hysteresis band at the extreme operating limits of the accumulator, in order to ensure that the intermittent operation of the accumulator is reduced.
- Applying an optimal operation control strategy using a mathematical simulation model and its feasibility in a real-world process.
- Adapting the proposed optimal methodology to the mathematical model requirements so that it can be applied and implemented without the requirement for modification of the mathematical model.
- Ensuring compatibility of the proposed methodology with common embedded systems commonly used in existing units, enabling its implementation in such systems.

To address the increased strain on the subsystems caused by frequent start-ups and shutdowns, a proposal has been made to employ a hysteresis band at the extreme limits of the state of charge. As has been found, this hysteresis band protects the

accumulator from a high number of charge/discharge cycles, while ensuring a reduction of continuous start/stops of the fuel cell and the electrolyzer. As a result, it helps to decrease the operation and maintenance costs.

The hysteresis band is defined as follows:

$$\left. \begin{aligned} HB_{acc} &= SOC_{mac,charge} - SOC_{max} \\ HB_{elec} &= SOC_{max} - SOC_{elec} \end{aligned} \right\} \quad (3.1)$$

Table 3.1 Explanation of the limits of the state of charge (SOC).

Limits SOC	Explanation of the limits SOC
SOC_{elec}	Minimum permissible operating limit for the electrolyzer
SOC_{max}	Maximum permissible operating limit of the electrolyzer
$SOC_{max,charge}$	Maximum acceptable load limit (with the hysteresis band)

Table 3.2 Explanation of the power limits of the electrolysis device.

Limits of the electrolysis device	Explanation of the power limits
P_{elec}	Power consumption of the electrolyzer
$P_{max,elec}$	Maximum power limit of the electrolyzer
$P_{min,elec}$	Minimum power limit of the electrolyzer

Energy Control strategy

When $P > 0$ and

- $SOC \geq SOC_{max,charge}$

If the available power falls within the operating limits of the electrolyzer ($P_{min,elec} \leq P \leq P_{max,elec}$), it will be fully utilized by the electrolyzer. In case the available

power exceeds $P_{\max,elec}$, the electrolyzer will utilize the maximum available power and the surplus power ($P - P_{\max,elec}$) will be rejected. Similarly, if the available power is lower than the minimum limit $P_{\min,elec}$, the accumulator will discharge power equivalent to $P_{\min,elec} - P$ in order to operate the electrolysis device at its minimum power limit.

- **$SOC_{\max} < SOC < SOC_{\max,charge}$ and $P < P_{\min,elec}$**

To ensure the operation of the electrolysis device at its minimum limit, the accumulator discharges power equivalent to $P_{\min,elec} - P$.

- **$SOC_{\max} < SOC < SOC_{\max,charge}$ and $P > P_{\max,elec}$**

The electrolyzer consumes power equal to $P_{\max,elec}$ and any excess power is directed towards charging the accumulator. Charging continues until the upper limit $SOC_{\max,charge}$ is reached, beyond which, no further charging is allowed and any excess charge is discharged.

- **$SOC_{\max} < SOC < SOC_{\max,charge}$ and $P_{\min,elec} \leq P \leq P_{\max,elec}$**

Full coverage of hydrogen production from photovoltaics.

- **$SOC_{elec} \leq SOC \leq SOC_{\max}$**

The operation of the electrolyzer depends on the previous time step of the simulation. If in the previous step (t-1), it was running and there is still excess power (P), it will continue to operate until the SOC reaches the SOC_{elec} limit. Once the SOC falls below this limit the accumulator cannot be discharged further and the operation of the electrolyzer will be terminated. If the electrolysis device is not operating, then the available power will be used entirely for charging the accumulator.

- **$SOC < SOC_{elec}$**

The accumulator is charged by the RES.

When $P < 0$

Full coverage of the necessary energy is obtained from the battery until it is discharged.

Chapter 4: Application and results of the energy control strategy

The primary goal of the operational algorithm and the adopted strategy is to maximize the efficient utilization of the generated energy. To achieve this, the following steps were taken:

- Selection of two regions for photovoltaic panel installation
- Collection of meteorological data (air temperature and solar radiation)
- Establishment of communities in each studied region
- Creation of energy profiles for the specific communities
- Definition of a specific hydrogen production target
- Optimization of the objective function using the optimtool
- Determining the selling price of hydrogen using Net Present Value (NPV)

The system was simulated using the Simulink environment in Matlab, and simulations used meteorological data from two regions in Crete, **namely Anogia and Tavronitis**. The meteorological data required for this thesis include air temperature and solar radiation values for each hour of the day, for a period of one year, in both regions.

For each studied region, two scenarios were examined regarding the energy needs of a community, which differed based on the presence or absence of a house. Community 1 consisted of hydrogen production only, while Community 2 included one house and hydrogen production. Subsequently, for each scenario, three successive optimization scenarios were studied for a specific hydrogen production target, progressively increasing as follows (at the end of the year):

Scenario 1: Hydrogen production target of 2000000It

Scenario 2: Hydrogen production target of 20000000It

Scenario 3: Hydrogen production target of 200000000It

To better understand the employed scenarios, a short diagram is presented below:

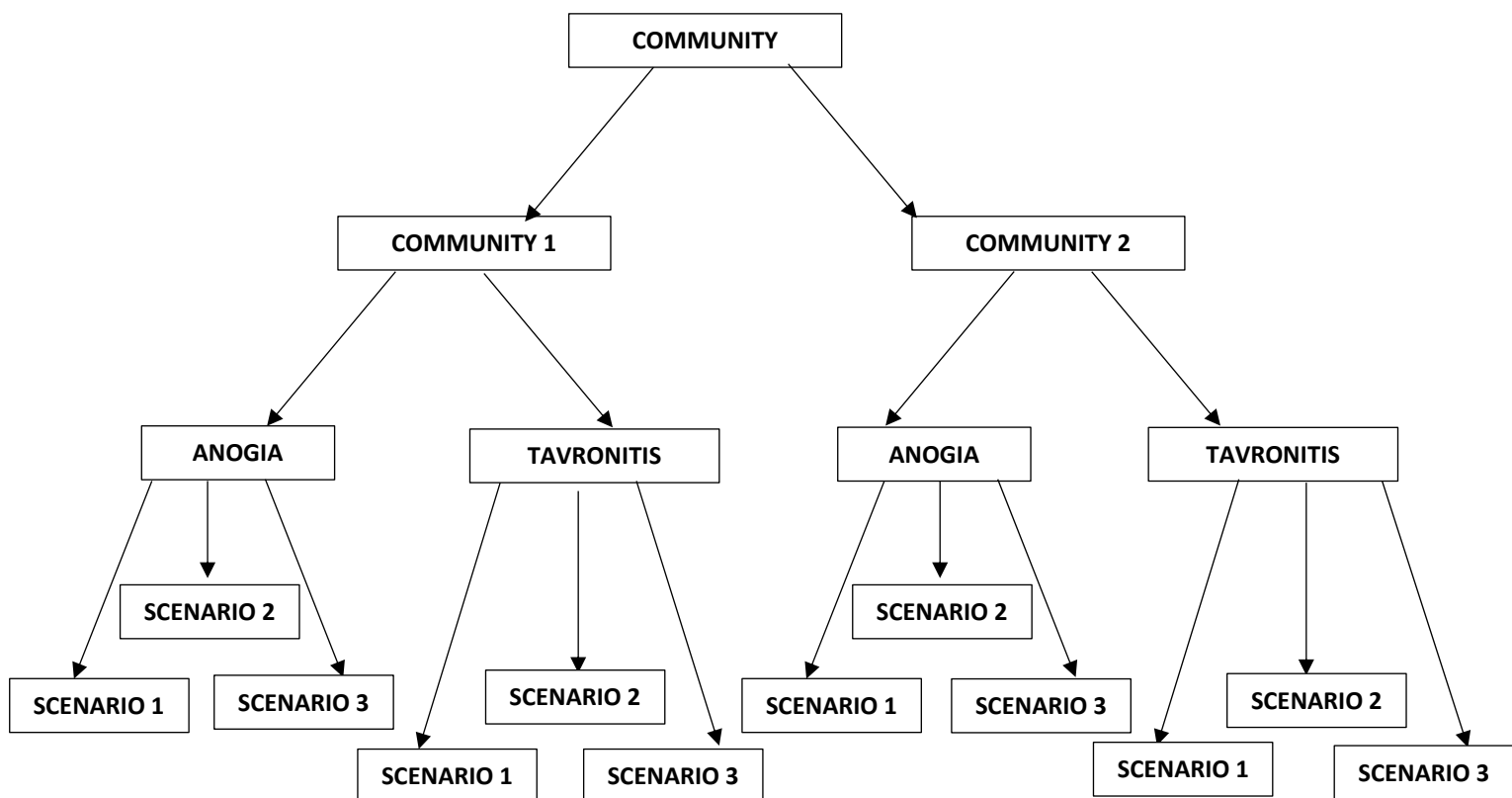


Diagram 4.1 Explanation of the employed scenarios.

Below, in tables 4.1 and 4.2, the average values of temperature and solar radiation for the areas of Anogia and Tavronitis, respectively, are presented, calculated using Excel.

Table 4.1 Average values of radiation and air temperature for one year in Anogia.

	Jan	Feb	Mar	Apr	May	Jun	Jul	Aug	Sep	Oct	Nov	Dec
Air Temperature [C°]	3.4	5.4	3.4	14.1	16.3	19.9	21	20.9	18.8	13.6	10.9	9.4
Solar Radiation [W/m²]	86.5	124.1	134.7	270.4	301.1	320	336.5	280.1	232.1	144.9	123.7	98.4

Table 4.2 Average values of radiation and air temperature for one year in Tavroniti.

	Jan	Feb	Mar	Apr	May	Jun	Jul	Aug	Sep	Oct	Nov	Dec
Air Temperature [C°]	9.1	9.9	9.1	15.9	19.5	24.5	25.6	25.5	22.7	18.5	16	14.3
Solar Radiation [W/m²]	68.7	105.7	111.5	215.8	242.4	275.1	266.8	226.1	193.3	115.1	101.8	75.8

Before presenting the optimization results, figures 4.1 and 4.2 for Anogia and 4.3 and 4.4 for Tavroniti, derived from the study system and MATLAB software, are presented. These figures refer to the meteorological data upon which all calculations for the following scenarios were based.

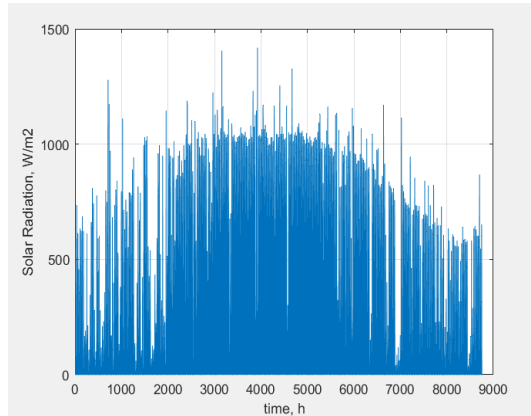


Figure 4.1 Solar radiation in Anogia throughout the year.

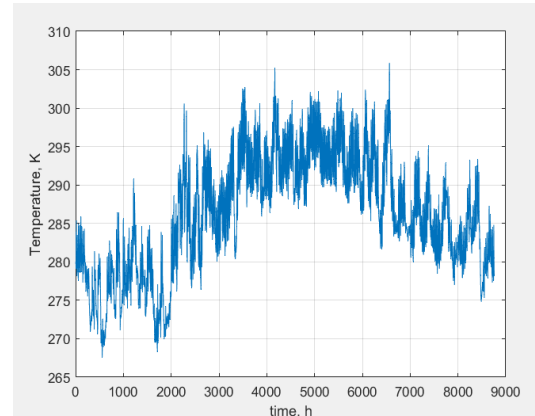


Figure 4.2 Air temperature in Anogia throughout the year.

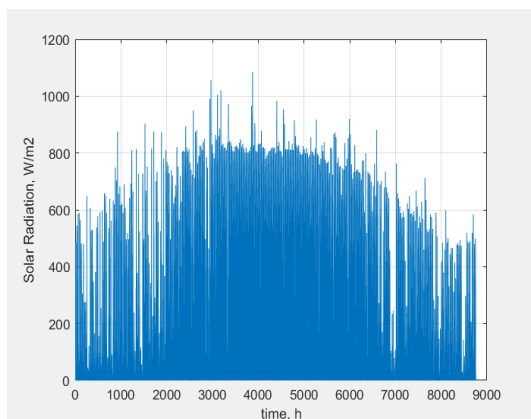


Figure 4.3 Solar radiation in Tavroniti throughout the year.

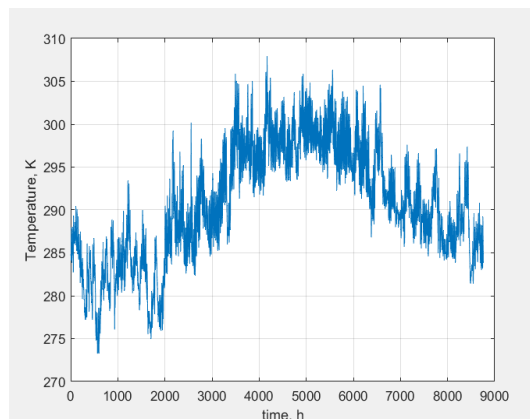


Figure 4.4 Air temperature in Tavroniti throughout the year.

The equations used in the optimization objective function are presented below:

- **Equipment cost equation (capital expenses, CAPEX)**

$$C_{\text{equipment}} = (\text{Number of PV} * 18000) + (\text{Number of ELEC} * 4000) + (\text{Number of BAT} * 500) + (\text{Number of TANK} * 200) \quad (4.1)$$

Table 4.3 Unit costs of the subsystems.

Unit Costs		
PV	18000€	10kW
ELECTROLYZER	4000€	6.9kW
BATTERY	500€	500Ah
TANK	200€	500lt

- **Equation for operational expenses**

$$C_{PV} = \text{Number of PV} * 100$$

$$C_{ELEC} = \text{Number of ELEC} * 500$$

$$C_{BAT} = \text{Number of BAT} * 10$$

$$C_{TANK} = \text{Number of TANK} * 10$$

Table 4.4 Operational costs of the subsystems.

Operational Costs		
PV	100€	10kW
ELECTROLYZER	500€	6.9kW
BATTERY	10€	500Ah
TANK	10€	500lt

- **Equation for profit through the sale of hydrogen and energy**

$$C_{SELLING} = (\text{Profit through the sale of hydrogen} * \text{Total hydrogen production}) + (\text{Profit through the sale of surplus energy} * \text{Total surplus energy}) \quad (4.2)$$

- **Equation for Net Present Value (NPV) for a repayment period of 20 years**

$$NPV(i) = NPV(i - 1) + \frac{(C_{PV} + C_{ELEC} + C_{BAT} + C_{TANK} - C_{SELLING})}{(1+h)^i} \quad (4.3)$$

Where:

i: Refers to successive years during the repayment period.

The calculation of NPV starts from the second year (*i* =2), as for the first year it is valied that $NPV(i =1) = C_{equipment}$.

h: Interest rate set to 0.06.

- **Objective minimisation/optimization function**

$$S_1 = ((\text{Total Hydrogen Production} - \text{Target Hydrogen Production})^2)$$

$$S_2 = (C_{equipment} - 10000)^2$$

$$S_3 = (\text{Total excess energy} - 1000)^2$$

$$S = S_1 + S_2 + S_3$$

Therefore, the objective function involves:

1. Achieving specific targets for hydrogen production at the end of each year (term S_1).
2. Minimizing equipment costs (term S_2).
3. Achieving zero energy loss (term S_3). In case of energy loss, i.e., surplus energy, this quantity can be sold.

4.1 Scenarios for covering the energy needs of Community 1

As mentioned at the beginning of this chapter, Community 1 consisted of hydrogen production only. Next, three optimization scenarios were examined successively, each with an increasing hydrogen production target. Specifically:

Scenario 1: Hydrogen production target of 2000000It

Scenario 2: Hydrogen production target of 20000000It

Scenario 3: Hydrogen production target of 200000000It

For the optimization section, the genetic algorithm optimization method was employed using Matlab to determine the optimal sizes of the subsystems. The Optimization Tool (optimtool) was utilized to obtain the final optimal values for photovoltaics, batteries and electrolysis unit. This ensures that the system can meet the energy needs of Community 1 while simultaneously achieving the predefined hydrogen (H₂) production target by the end of each year. The input values provided to the Optimization Tool are the same for both regions and define the boundaries within which the optimal values should fall. These boundaries vary depending on the hydrogen production target scenario. In all scenarios, the Genetic Algorithm is designated as the solver, and the PMS2_no_comp_load_Opt_v1 function is specified for optimization. Finally, the number of variables resulting from the Optimization Tool is set to 5. The first three are represented as $\text{opt} = [a, b, c]$, while the remaining two constraints define the lower and upper bounds of the battery's state of charge. These constraints, however, are not included in the objective function and they are defined simply for the optimal operation of the optimization process. Specifically:

- **a**: Optimal size of photovoltaics

- **b**: Optimal size of batteries
- **c**: Optimal size of electrolyzer

For Scenario 1, with a hydrogen production target of 2000000 liters, the following steps were taken:

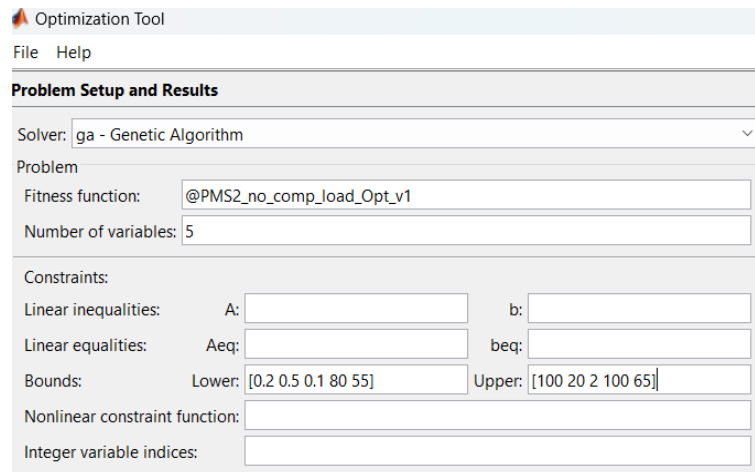


Figure 4.5 Finding optimal values for the first scenario for hydrogen production target.

After obtaining the optimal values using the optimization tool, which relate to the previously mentioned parameters, the mathematical code is implemented using the target variables specific to Scenario 1 of hydrogen production. This includes the required hydrogen storage, the required hydrogen production, and the resulting hydrogen selling price from the optimization.

Moving forward we repeated the same steps for Scenario 2, where the hydrogen production target was set at 20000000 liters, and for Scenario 3, with a hydrogen production target of 200000000 liters. In these scenarios, we increased the upper limits of the variables a, b, and c, while keeping the variables that define the lower and upper bounds of the battery's state of charge unchanged.

4.2 Scenarios for covering the energy needs of Community 2

As previously mentioned in this chapter, Community 2 included one house and hydrogen production. Then, three optimization scenarios were examined successively, each with an increasing hydrogen production target. These scenarios were as follows:

Scenario 1: Hydrogen production target of 2000000lt

Scenario 2: Hydrogen production target of 20000000lt

Scenario 3: Hydrogen production target of 20000000lt

Subsequently, the Optimization Tool (optimtool) is used in order to determine the final optimal values for photovoltaics, batteries and electrolysis unit. These values were selected to meet the energy demands of Community 2 while simultaneously achieving the predefined hydrogen (H₂) production target by the end of each year.

For Scenario 1, which had a hydrogen production target of 2000000lt the following steps were taken:

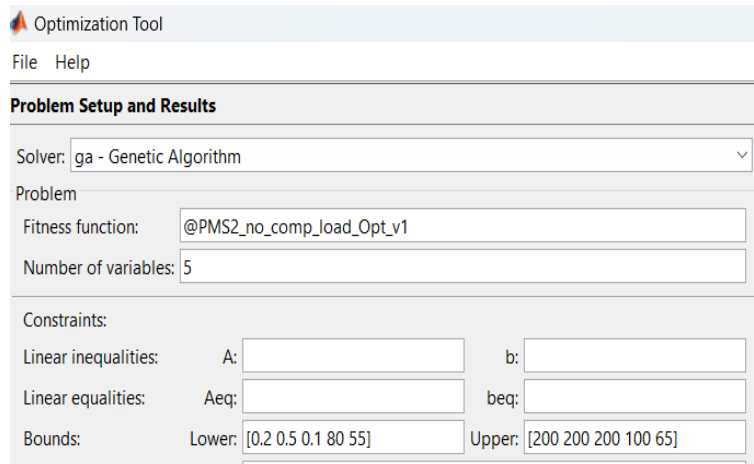


Figure 4.6 Finding optimal values for the first scenario for hydrogen production target.

After obtaining the optimal values through optimization tool, which are related to the parameters mentioned earlier, the mathematical code is implemented using the target variables specific to Scenario 1 for hydrogen production. This includes the required hydrogen storage, the necessary hydrogen production, and the resulting hydrogen selling price a_w optimized.

Subsequently, the same steps were followed for Scenario 2, which had a hydrogen production target of 20000000 liters, and for Scenario 3, with a hydrogen production target of 200000000 liters. This involved increasing the upper limits of the variables a , b , and c while keeping the variables that define the lower and upper bounds of the battery's state of charge unchanged.

4.3 Recording of results for the energy needs coverage scenarios of community 1

As mentioned at the beginning of this chapter, Community 1 consists of hydrogen production only.

4.3.1 Use of data from the area of Anogia

The table below presents the results obtained during the implementation of the scenario for meeting the energy needs of community 1, regarding the characteristics of the respective hydrogen production target scenarios. Specifically:

- **Number (or size) of PV, Number (or size) of BAT, Number (or size) of ELEC, Number (or size) of TANK:** refers to the size of the photovoltaic panels, batteries, electrolyzer, and tanks that emerged as the optimal solution for achieving each target scenario, multiplied by the corresponding nominal size as indicated for each scenario.
- **Hydrogen production:** refers to the total hydrogen production obtained by the end of the year, aiming to achieve each mentioned scenario target (2000000 liters, 20000000 liters, and 200000000 liters).
- **Hydrogen selling price:** refers to the break-even price, which is the selling price of hydrogen required to offset the expenses incurred for equipment purchase, so that the net present value (NPV) at the end of the 20-year period becomes zero. After this point, the project will generate profit. In the calculation equation of the net present value, the values we don't know are the $C_{SELLING}$ and the NPV(i) for each year. For each scenario, various tests are conducted in the code by adjusting the profit through the sale of hydrogen (changing $C_{SELLING}$) to achieve a NPV break-even point zeroing after 20 years. The equations explaining these concepts are (4.2) and (4.3).

Table 4.5 Results concerning the system simulated in Anogia.

	Scenario 1	Scenario 2	Scenario 3
Size of PV, kW	6.9	70.8	638.8
Size of BAT, Ah	844.2	6865.5	119660.6
Size of ELEC, kW	8.4	51.9	838.7
Size of TANK, m³	20	200	2000
Hydrogen production, lt	2000000	20003000	199980000
Hydrogen selling price, €	16.8	15.3	15.9

Next, Figure 4.7 is presented, which depicts the hydrogen selling prices (in €) per production target scenario.

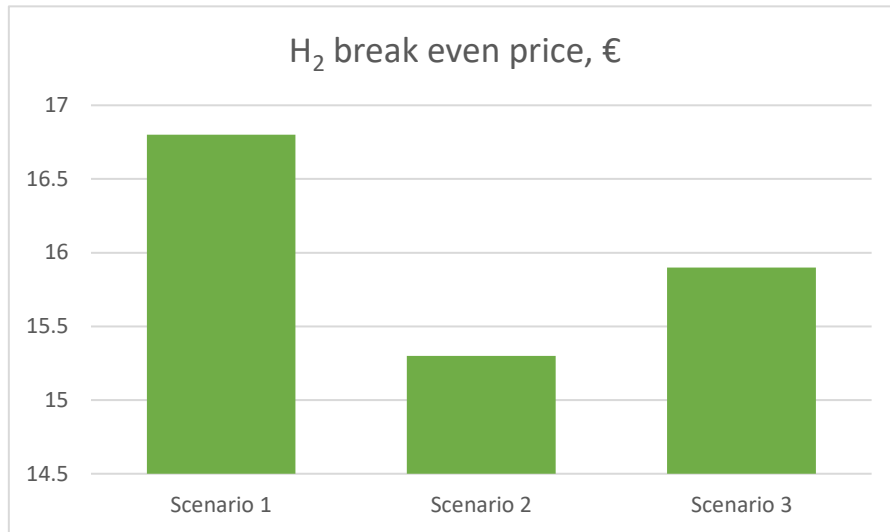


Figure 4.7 Hydrogen sales prices (€) per production target scenarios.

Then, Figures 4.(8-10) are presented sequentially, corresponding to scenarios 1 to 3. The figures refer to the quantity of hydrogen achieving the respective target of scenarios 1 to 3.

Quantity of hydrogen achieving the respective target:

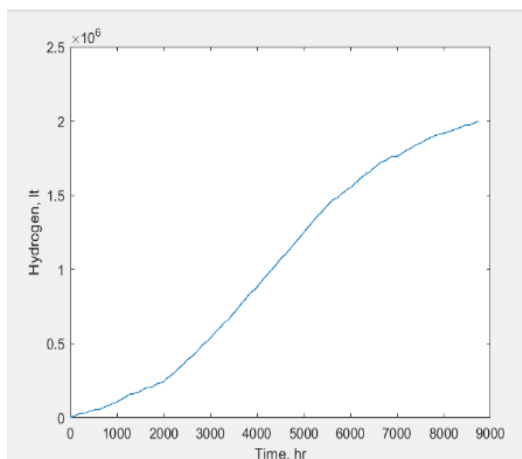


Figure 4.8 Scenario 1

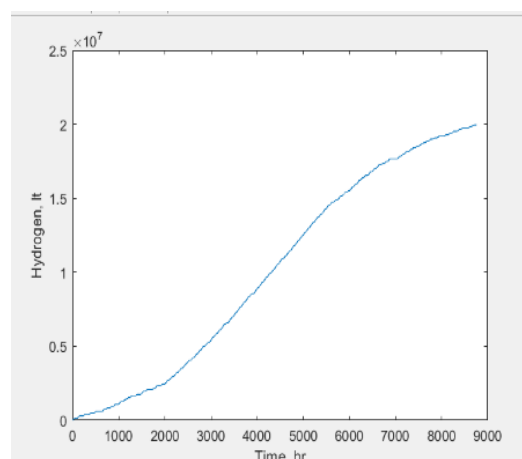


Figure 4.9 Scenario 2

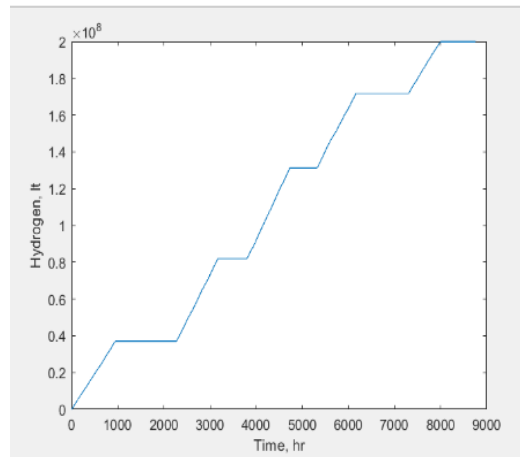


Figure 4.10 Scenario 3

As shown above, the target is achieved in all hydrogen production scenarios. We observe that in all production scenarios, the required quantities are achieved with a continuous increase. In both the first and second scenarios, production seems to be achieved with greater stability in the rate, while in the third scenario, there is a greater decrease in hydrogen production stability.

The table below shows the results obtained during the implementation of the scenario for covering the energy needs of community 1, regarding the operation of the battery and the electrolyzer, respectively, for each hydrogen production target scenario. In more detail:

- **Battery charging time:** refers to the percentage of time the battery was charging.
- **Battery discharging time:** refers to the percentage of time the battery was discharging.
- **Electrolyzer operating time:** refers to the percentage of time the electrolyzer was operating.

Table 4.6 Capturing results regarding the operation of the battery and electrolyzer of the simulated system in Anogia.

	Scenario 1	Scenario 2	Scenario 3
Battery charging time, %	19.5	27	24.8
Battery discharging time, %	19.5	40.7	36.8
Electrolyzer operating time,%	37.4	60.4	49.1

Next, Figures 4.(11-13) are presented sequentially, corresponding to scenarios 1 to 3. These figures depict the battery charge status as presented in hydrogen production target scenarios 1 to 3.

Battery charge status:

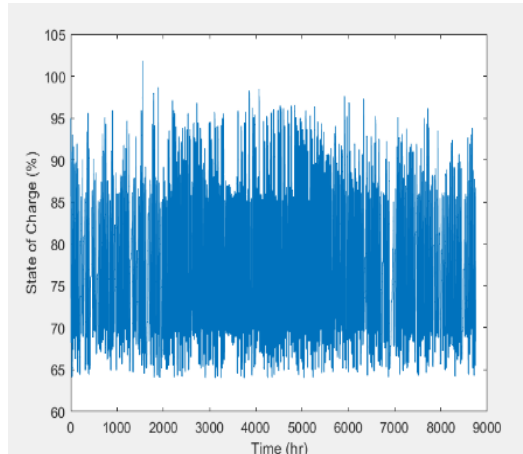


Figure 4.11 Scenario 1

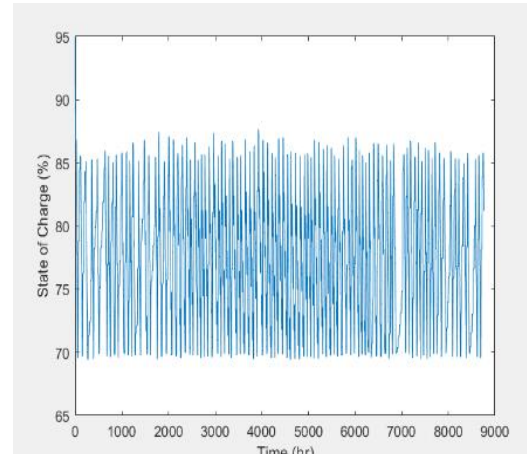


Figure 4.12 Scenario 2

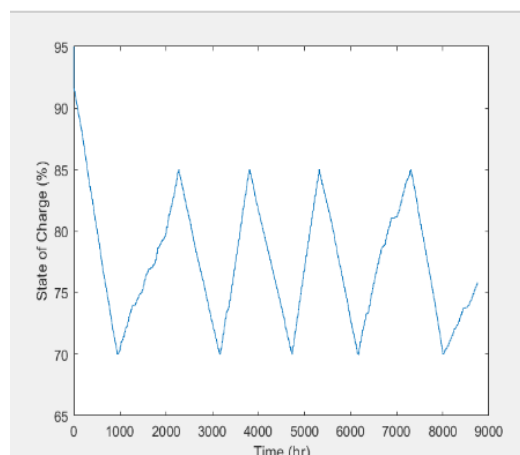


Figure 4.13 Scenario 3

The charging and discharging rates of the battery are higher in the second hydrogen production scenario, while they are lower in the first scenario. It is also observed that the battery charging cycles decrease as the required quantity of hydrogen production increases, which is why more charging cycles of the battery are achieved in the first scenario.

The figure below presents the results obtained during the implementation of the scenario for covering the energy needs of community 1, regarding the final energy amounts for each hydrogen production target scenario. In more detail:

- **Energy provided by the battery to the electrolyzer:** refers to the total energy provided by the battery for the operation of the electrolyzer until the end of the year.

- **Energy provided by renewable energy sources (RES) to the battery:** refers to the total energy provided by the photovoltaic panels for charging the battery until the end of the year.
- **Energy provided by renewable energy sources (RES) to the electrolyzer:** refers to the total energy provided by the photovoltaic panels for the operation of the electrolyzer until the end of the year.
- **Lost energy:** refers to the total surplus energy that is not utilized and is lost from the system until the end of the year (0% in all scenarios).

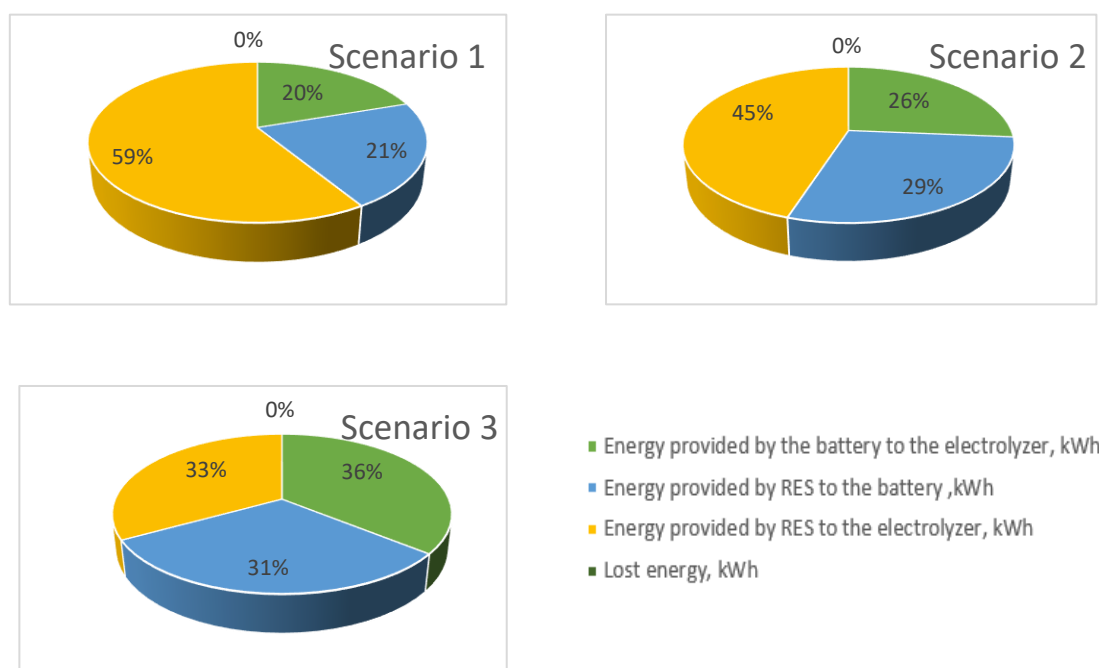


Figure 4.14 Representation of results regarding the final energy amounts in Anogia.

4.3.2 Use of data from the area of Tavroniti

The table below presents the results obtained during the implementation of the scenario for covering the energy needs of community 1, regarding the characteristics of the respective hydrogen production target scenarios. More specifically:

- **Number (or size) of PV, Number (or size) of BAT, Number (or size) of ELEC, Number (or size) of TANK:** refers to the size of the photovoltaic panels, batteries, electrolyzer, and tanks that emerged as the optimal solution for achieving each target scenario, multiplied by the corresponding nominal size as indicated for each scenario.

- **Hydrogen production:** refers to the total hydrogen production obtained by the end of the year, aiming to achieve each mentioned scenario target (2000000 liters, 20000000 liters, and 200000000 liters).
- **Hydrogen selling price:** refers to the break-even price, which is the selling price of hydrogen required to offset the expenses incurred for equipment purchase, so that the net present value (NPV) at the end of the 20-year period becomes zero. After this point, the project will generate profit.

Table 4.7 Results concerning the system simulated in Tavroniti.

	Scenario 1	Scenario 2	Scenario 3
Size of PV, kW	8.8	84.5	837.2
Size of BAT, Ah	1740.6	21487.1	89208.1
Size of ELEC, kW	9.1	129.8	586.5
Size of TANK, m³	20	200	2000
Hydrogen production, lt	2000000	20000000	200000000
Hydrogen selling price, €	20.3	21.6	17.7

Next, Figure 4.15 is presented, which depicts the hydrogen selling prices (in €) per production target scenario.

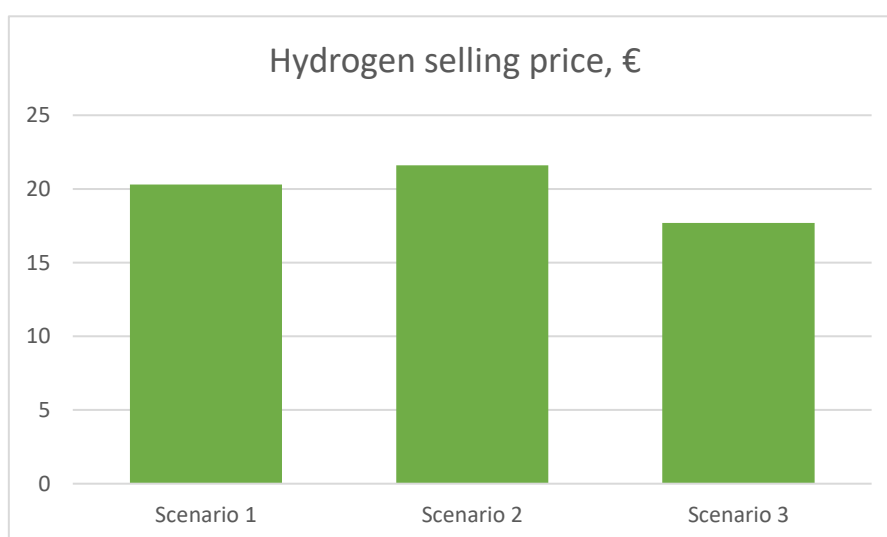


Figure 4.15 Hydrogen sales prices (€) per production target scenario.

Then, Figures 4.(15-17) are presented sequentially, corresponding to scenarios 1 to 3. The figures refer to the quantity of hydrogen achieving the respective target of scenarios 1 to 3.

Quantity of hydrogen achieving the respective target:

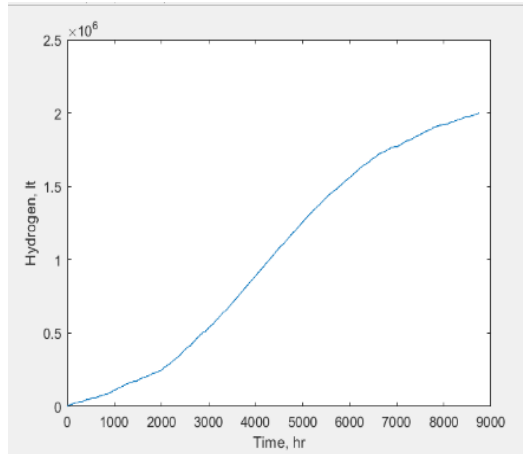


Figure 4.15 Scenario 1

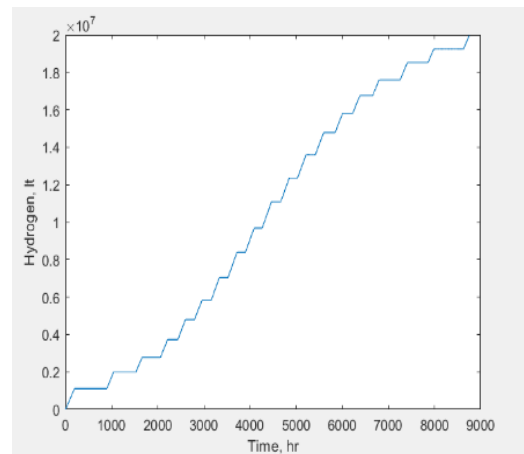


Figure 4.16 Scenario 2

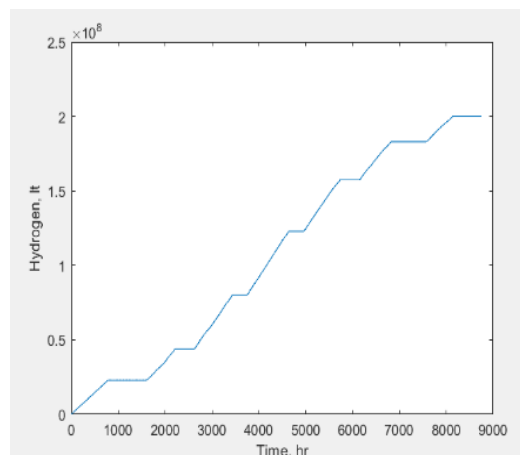


Figure 4.17 Scenario 3

As shown above, in all hydrogen production scenarios, the target is achieved. We observe that the production reaches the initial goal of 2000000 liters with a continuous increase. However, as the required production quantity increases, there is a gradual decrease in the stability of hydrogen production, as seen in the last two scenarios where production is interrupted for some hours during the year.

The table below shows the results obtained during the implementation of the scenario for covering the energy needs of community 1, regarding the operation of the battery and the electrolzer, respectively, for each hydrogen production target scenario. In more detail:

- **Battery charging time:** refers to the percentage of time the battery was charging.
- **Battery discharging time:** refers to the percentage of time the battery was discharging.
- **Electrolyzer operating time:** refers to the percentage of time the electrolyzer was operating.

Table 4.8 Capturing results regarding the operation of the battery and electrolyzer of the simulated system in Tavroniti.

	Scenario 1	Scenario 2	Scenario 3
Battery charging time, %	31.7	31.2	23.1
Battery discharging time, %	36.7	28.1	40.1
Electrolyzer operating time,%	46.7	35.9	57.9

Next, Figures 4.(18-20) are presented sequentially, corresponding to scenarios 1 to 3. These figures depict the battery charge status as presented in hydrogen production target scenarios 1 to 3.

Battery charge status:

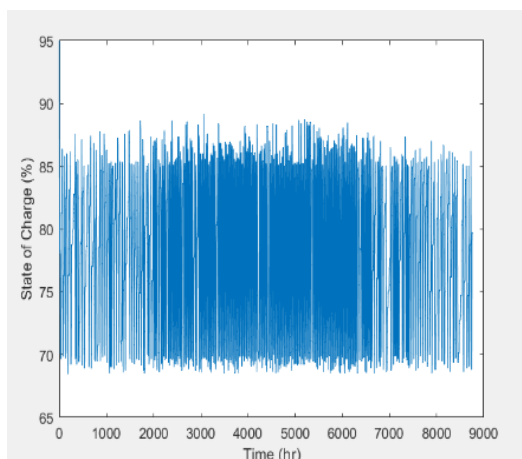


Figure 4.18 Scenario 1

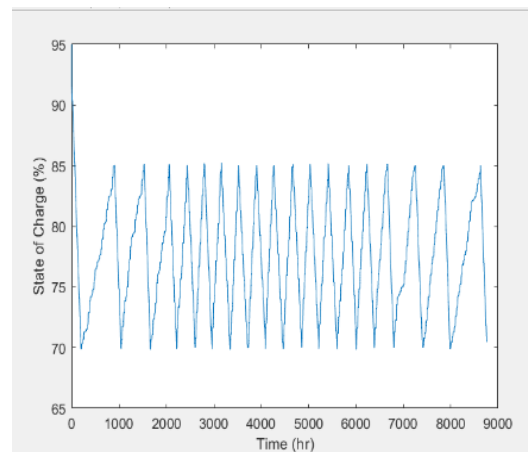


Figure 4.19 Scenario 2

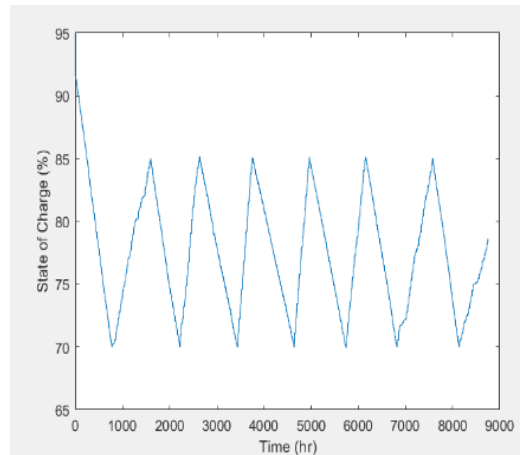


Figure 4.20 Scenario 3

The charging and discharging rates of the battery are very frequent in the first hydrogen production scenario, achieving the most charging cycles during a year. It is also observed that the battery charging cycles decrease as the required quantity of H₂ production increases.

The figure below presents the results obtained during the implementation of the scenario for covering the energy needs of community 1, regarding the final energy amounts for each hydrogen production target scenario. In more detail:

- **Energy provided by the battery to the electrolyzer:** refers to the total energy provided by the battery for the operation of the electrolyzer until the end of the year.
- **Energy provided by renewable energy sources (RES) to the battery:** refers to the total energy provided by the photovoltaic panels for charging the battery until the end of the year.
- **Energy provided by renewable energy sources (RES) to the electrolyzer:** refers to the total energy provided by the photovoltaic panels for the operation of the electrolyzer until the end of the year.
- **Lost energy:** refers to the total surplus energy that is not utilized and is lost from the system until the end of the year. (0% in all scenarios)

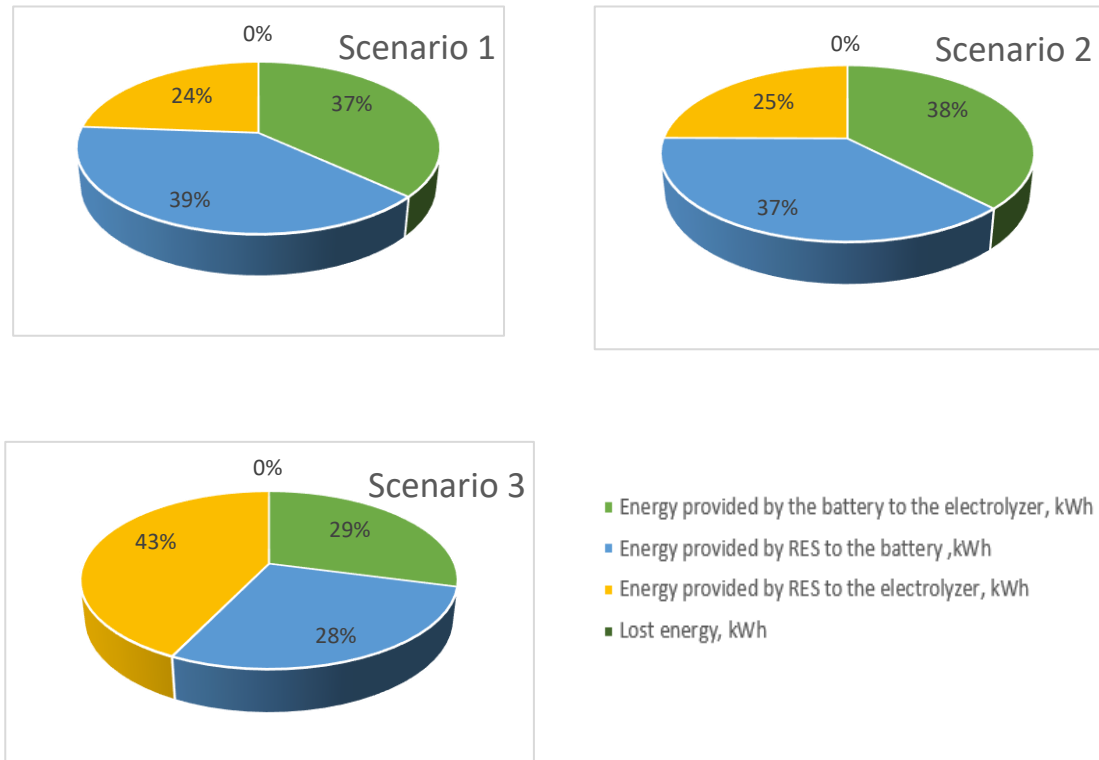


Figure 4.21 Representation of results regarding the final energy amounts in Tavroniti.

4.4 Recording of results for the energy needs coverage scenario of community 2

As mentioned at the beginning of this chapter, Community 2 includes houses and hydrogen production. The average energy load required for community 2 is 7.3 Kw and the energy load is shown below.

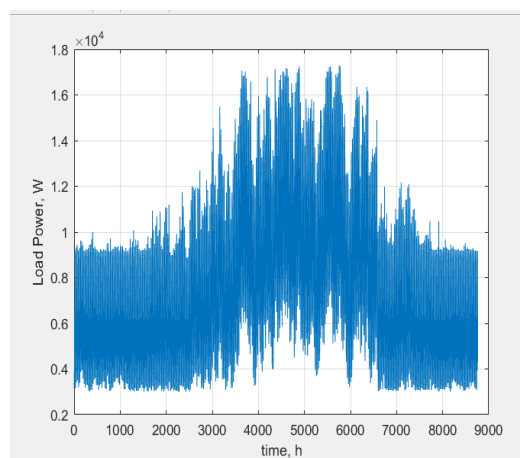


Figure 4.22 Energy load of Community 2.

4.4.1 Use of data from the area of Anogia

The table below presents the results obtained during the implementation of the scenario for covering the energy needs of community 2, concerning the characteristics of the respective hydrogen production target scenario. More specifically:

- **Number (or size) of PV, Number (or size) of BAT, Number (or size) of ELEC, Number (or size) of TANK:** refers to the size of the photovoltaic panels, batteries, electrolyzer, and tanks that emerged as the optimal solution for achieving each target scenario, multiplied by the corresponding nominal size as indicated for each scenario.
- **Hydrogen production:** refers to the total hydrogen production obtained by the end of the year, aiming to achieve each mentioned scenario target (2000000 liters, 20000000 liters, and 200000000 liters).
- **Hydrogen selling price:** refers to the break-even price, which is the selling price of hydrogen required to offset the expenses incurred for equipment purchase, so that the net present value (NPV) at the end of the 20-year period becomes zero. After this point, the project will generate profit.

Table 4.9 Results concerning the system simulated in Anogia.

	Scenario 1	Scenario 2	Scenario 3
Size of PV, kW	43.7	153.8	698.8
Size of BAT, Ah	30344.2	6865.5	119660.6
Size of ELEC, kW	8.5	51.9	838.7
Size of TANK, m³	20	200	2000
Hydrogen production, lt	2000000	20000000	200000000
Hydrogen selling price, €	60.8	22.8	16.7

Next, Figure 4.22 is presented, which depicts the hydrogen selling prices (in €) per production target scenario.

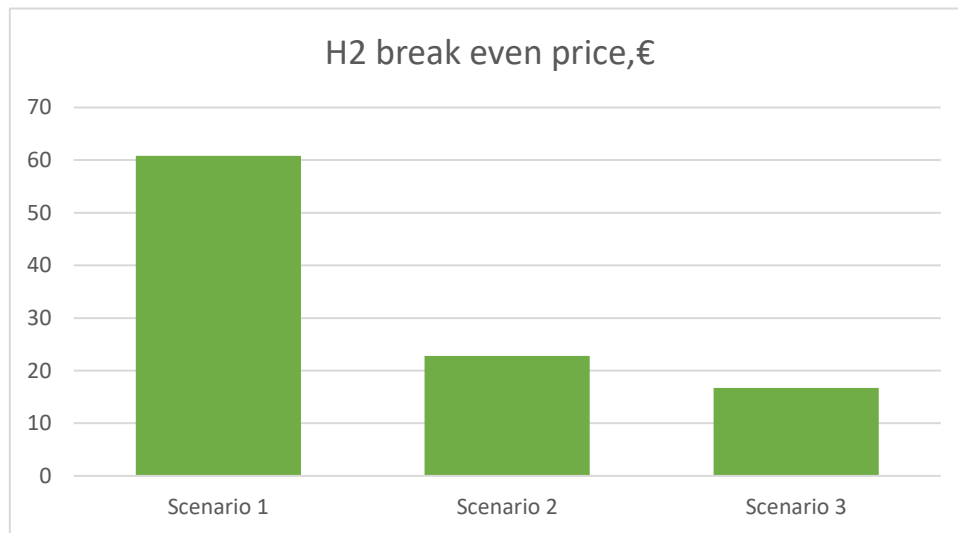


Figure 4.23 Hydrogen sales prices (€) per production target scenario.

Then, Figures 4.(24-26) are presented sequentially, corresponding to scenarios 1 to 3. The figures refer to the quantity of hydrogen achieving the respective target of scenarios 1 to 3.

Quantity of hydrogen achieving the respective target:

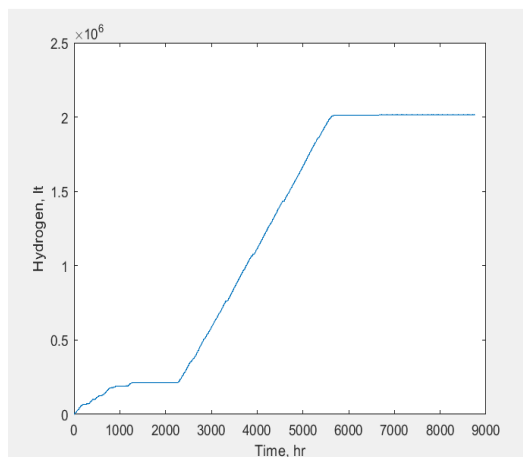


Figure 4.24 Scenario 1

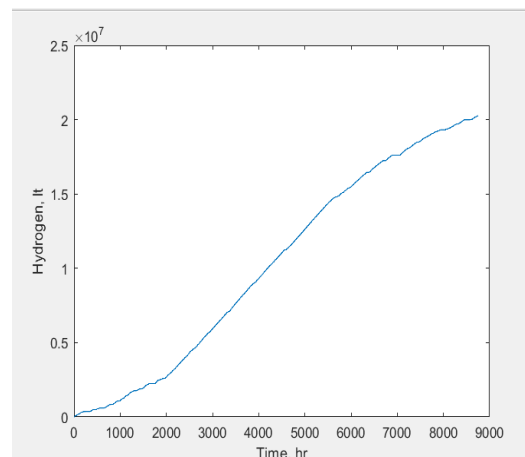


Figure 4.25 Scenario 2

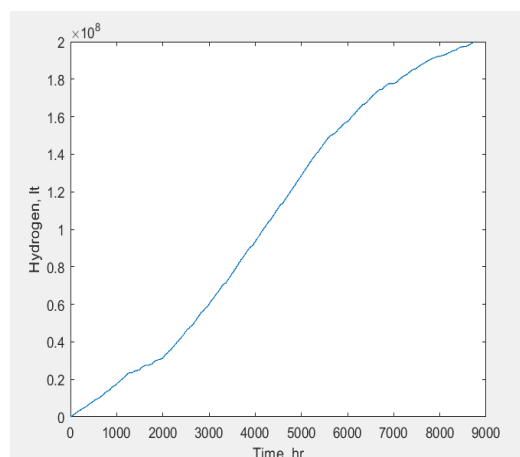


Figure 4.26 Scenario 3

As demonstrated above, in all hydrogen production scenarios, the predicted target are achieved. It is observed that in all production scenarios, the required quantities are achieved with a continuous increase. In the second and third scenarios, production seems to be achieved with greater stability in the rate, while in the first scenario, there is a greater reduction in the stability of hydrogen production.

The table below displays the results obtained during the implementation of the scenario for meeting the energy needs of community 2, concerning the operation of the battery and the electrolyzer, respectively, for each hydrogen production target scenario. In more detail:

- **Battery charging time:** refers to the percentage of time the battery was charging.
- **Battery discharging time:** refers to the percentage of time the battery was discharging.
- **Electrolyzer operating time:** refers to the percentage of time the electrolyzer was operating.

Table 4.10 Capturing results regarding the operation of the battery and electrolyzer of the simulated system in Anogia.

	Scenario 1	Scenario 2	Scenario 3
Battery charging time, %	25.5	14.4	15.2
Battery discharging time, %	69.9	63.2	65.5
Electrolyzer operating time,%	17.5	30.9	39.1

Next, Figures 4.(27-29) are presented sequentially, corresponding to scenarios 1 to 3. These figures depict the battery charge status as presented in hydrogen production target scenarios 1 to 3.

Battery charge status:

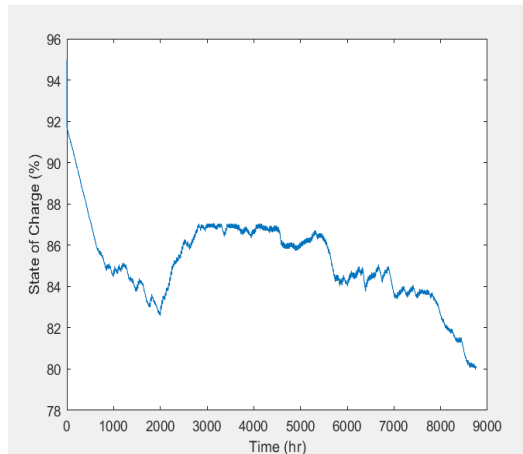


Figure 4.27 Scenario 1

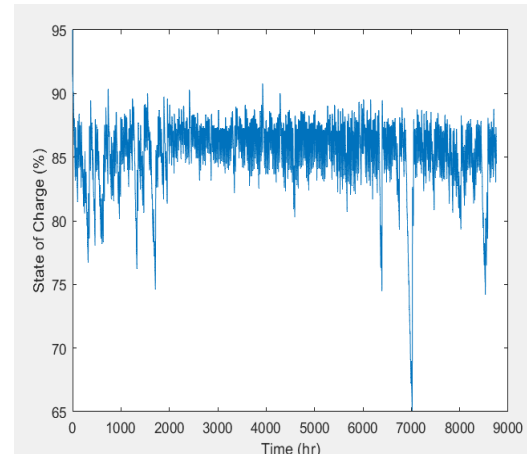


Figure 4.28 Scenario 2

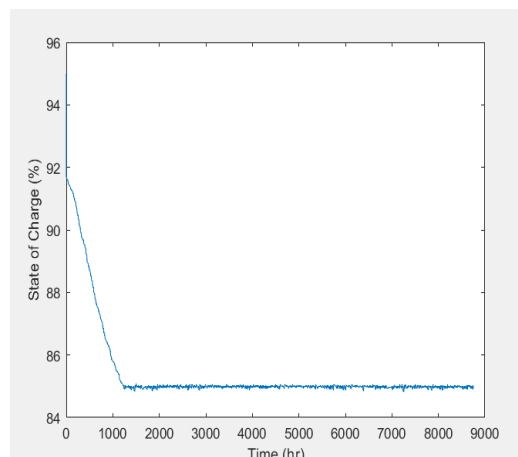


Figure 4.29 Scenario 3

The charging and discharging rate of the battery are very frequent in the second hydrogen production scenario, achieving the most charging cycles during a year. Fewer battery charging cycles, with the lowest frequency of charges and discharges, are reported in the third scenario with the highest required quantity of H₂ production.

The figure below presents the results obtained during the implementation of the scenario for meeting the energy needs of community 2, concerning the final energy amounts for each hydrogen production target scenario. In more detail:

- **Energy provided by the battery to the electrolyzer:** refers to the total energy provided by the battery for the operation of the electrolyzer until the end of the year.
- **Energy provided by renewable energy sources (RES) to the battery:** refers to the total energy provided by the photovoltaic panels for charging the battery until the end of the year.

- **Energy provided by renewable energy sources (RES) to the electrolyzer:** refers to the total energy provided by the photovoltaic panels for the operation of the electrolyzer until the end of the year.
- **Lost energy:** refers to the total surplus energy that is not utilized and is lost from the system until the end of the year (between 0-4% in all scenarios).

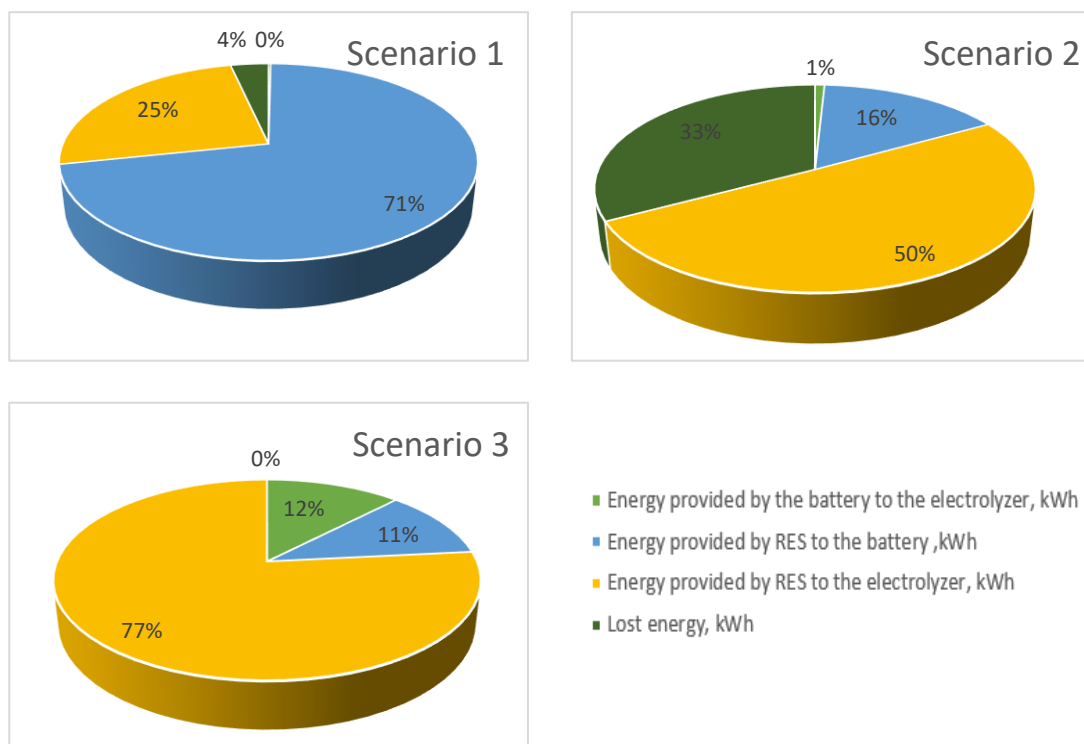


Figure 4.30 Representation of results regarding the final energy amounts in Anogia.

4.4.2 Use of data from the area of Tavroniti

The table below presents the results obtained during the implementation of the scenario for covering the energy needs of community 2, concerning the characteristics of the respective hydrogen production target scenario. More specifically:

- **Number (or size) of PV, Number (or size) of BAT, Number (or size) of ELEC, Number (or size) of TANK:** refers to the size of the photovoltaic panels, batteries, electrolyzer, and tanks that emerged as the optimal solution for achieving each target scenario, multiplied by the corresponding nominal size as indicated for each scenario.
- **Hydrogen production:** refers to the total hydrogen production obtained by the end of the year, aiming to achieve each mentioned scenario target (2000000 liters, 20000000 liters, and 200000000 liters).

- **Hydrogen selling price:** refers to the break-even price, which is the selling price of hydrogen required to offset the expenses incurred for equipment purchase, so that the net present value (NPV) at the end of the 20-year period becomes zero. After this point, the project will generate profit.

Table 4.11 Results concerning the system simulated in Tavroniti.

	Scenario 1	Scenario 2	Scenario 3
Size of PV, kW	55.1	132.4	897.2
Size of BAT, Ah	25240.6	21487	89208.1
Size of ELEC, kW	9.2	129.8	586.5
Size of TANK, m³	20	200	2000
Hydrogen production, lt	2000000	20000000	200000000
Hydrogen selling price, €	81.4	27.8	16.7

Next, Figure 4.31 is presented, which depicts the hydrogen selling prices (in €) per production target scenario.

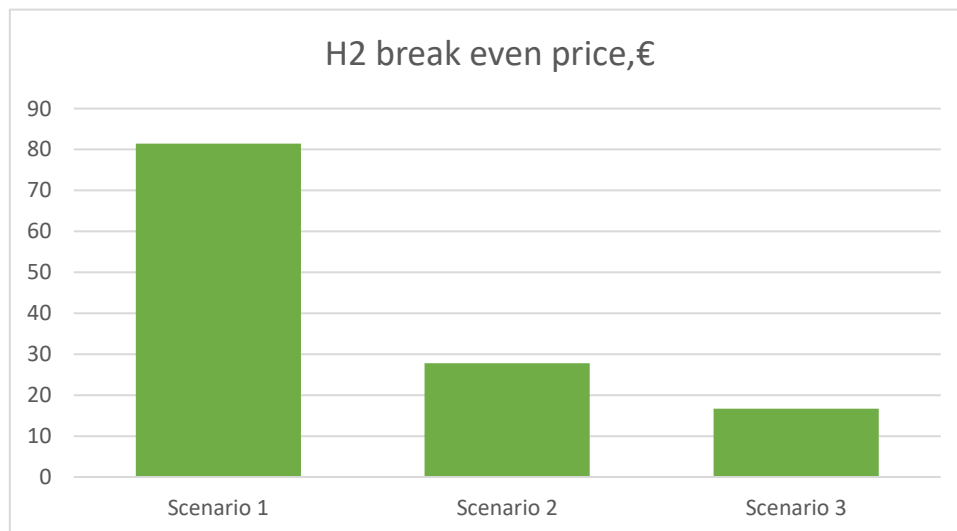


Figure 4.31 Hydrogen sales prices (€) per production target scenario.

Then, Figures 4.(32-34) are presented sequentially, corresponding to scenarios 1 to 3. The figures refer to the quantity of hydrogen achieving the respective target of scenarios 1 to 3.

Quantity of hydrogen achieving the respective target:

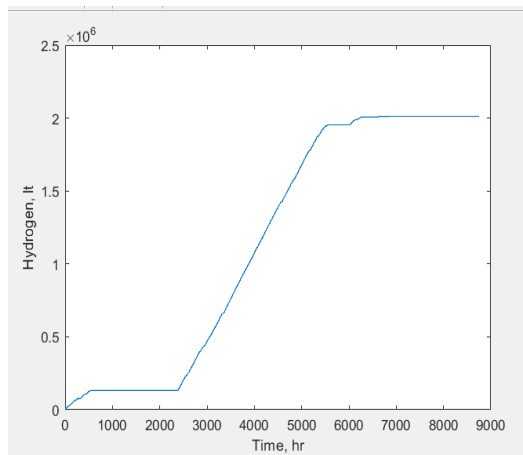


Figure 4.32 Scenario 1

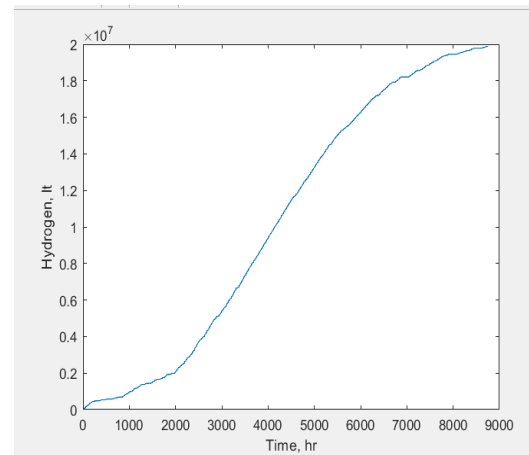


Figure 4.33 Scenario 2

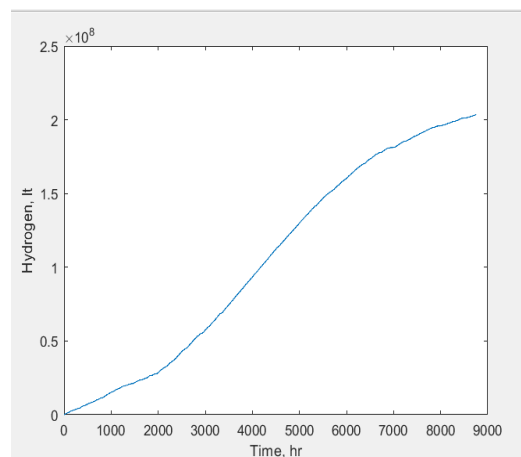


Figure 4.34 Scenario 3

As shown above, in all hydrogen production scenarios, the targeted production are achieved. As the required quantity of hydrogen production increases, there is a gradual increase in the stability of hydrogen production, as seen in the last scenario where production smoothness is notable.

The table below presents the results obtained during the implementation of the scenario for meeting the energy needs of community 2, concerning the operation of the battery and the electrolyzer, respectively, for each hydrogen production target scenario. In more detail:

- **Battery charging time:** refers to the percentage of time the battery was charging.
- **Battery discharging time:** refers to the percentage of time the battery was discharging.
- **Electrolyzer operating time:** refers to the percentage of time the electrolyzer was operating.

Table 4.12 Capturing results regarding the operation of the battery and electrolyzer of the simulated system in Tavroniti.

	Scenario 1	Scenario 2	Scenario 3
Battery charging time, %	26.1	16.1	14.3
Battery discharging time, %	69.2	67.7	65.3
Electrolyzer operating time,%	16.6	21.9	39.3

Next, Figures 4.(35-37) are presented sequentially, corresponding to scenarios 1 to 3. These figures depict the battery charge status as presented in hydrogen production target scenarios 1 to 3.

Battery charge status:

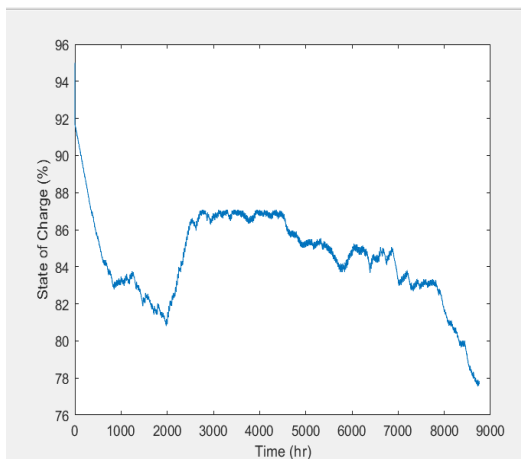


Figure 4.35 Scenario 1

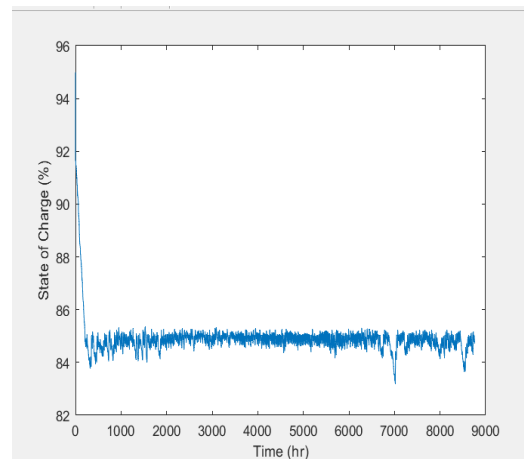


Figure 4.36 Scenario 2

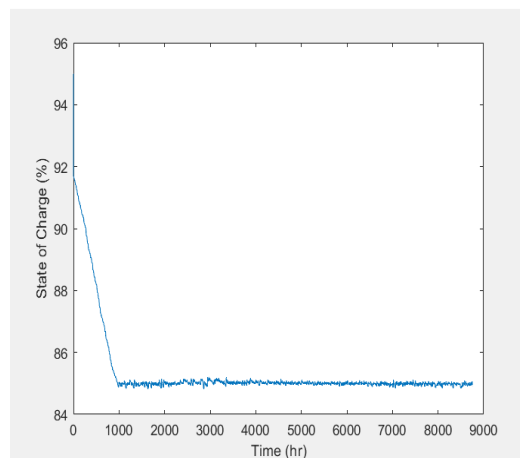


Figure 4.37 Scenario 3

The charging and discharging rates of the battery are very frequent in the second hydrogen production scenario, achieving the most charging cycles during a year.

The figure below presents the results obtained during the implementation of the scenario for covering the energy needs of community 2, regarding the final energy amounts for each hydrogen production target scenario. In more detail:

- **Energy provided by the battery to the electrolyzer:** refers to the total energy provided by the battery for the operation of the electrolyzer until the end of the year.
- **Energy provided by renewable energy sources (RES) to the battery:** refers to the total energy provided by the photovoltaic panels for charging the battery until the end of the year.
- **Energy provided by renewable energy sources (RES) to the electrolyzer:** refers to the total energy provided by the photovoltaic panels for the operation of the electrolyzer until the end of the year.
- **Lost energy:** refers to the total surplus energy that is not utilized and is lost from the system until the end of the year (between 0-4%).

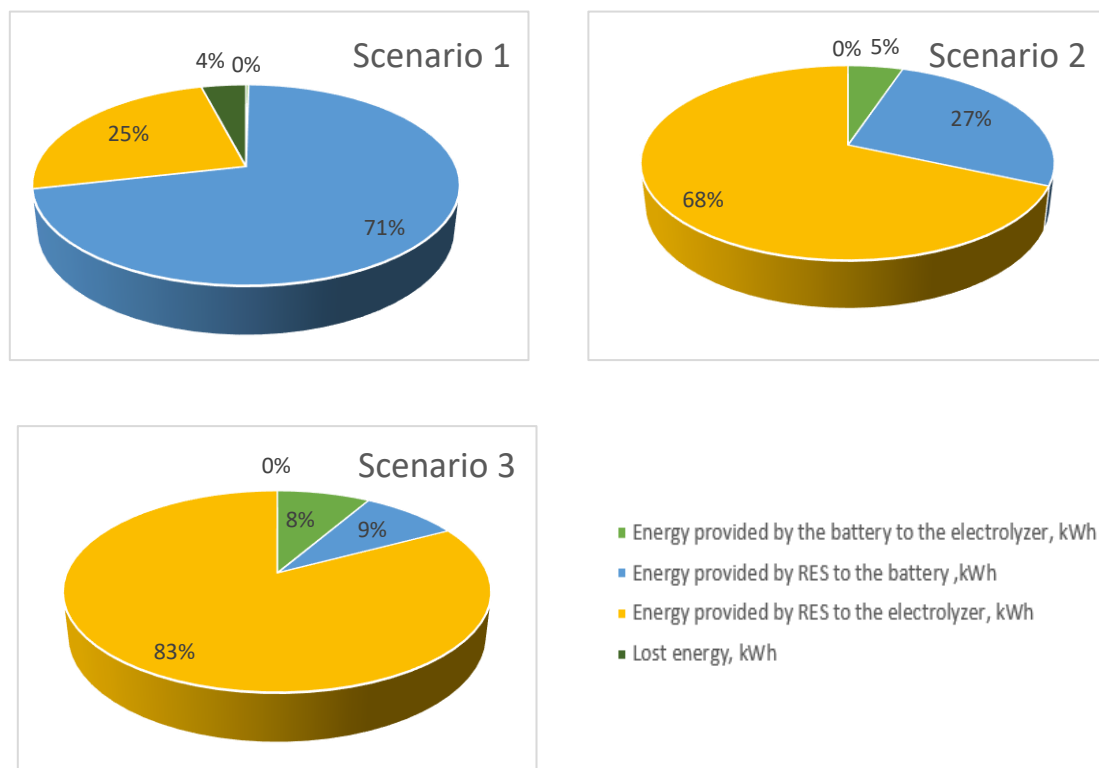


Figure 4.38 Representation of results regarding the final energy amounts in Tavroniti.

Chapter 5: Conclusions and Future Steps

For the study and simulation of the system examined in this thesis, meteorological measurements from the region of Anogia and Tavroniti were used. The initial objective of this thesis was to achieve the autonomy of the electricity production system from Renewable Energy Sources (RES). The aim was to ensure a continuous power supply to meet specific demand requirements while also utilizing surplus energy to produce hydrogen.

Community 1

Below are the results of the simulation for community 1, which consists of hydrogen production only. The results are both for the Anogia and the Tavroniti.

Table 5.1 Comparison of results concerning the system.

	Anogia			Tavronitis		
	Scenario 1	Scenario 2	Scenario 3	Scenario 1	Scenario 2	Scenario 3
Size of PV, kW	6.9	70.8	638.8	8.8	84.5	837.2
Size of BAT, Ah	844.2	6865.5	119660.6	1740.6	21487.1	89208.1
Size of ELEC, kW	8.4	51.9	838.7	9.1	129.8	586.5
Size of TANK, m ³	20	200	2000	20	200	2000
Investment cost, €	19140	172460	1835700	23781	256760	2016200
Hydrogen selling price, €	16.8	15.3	15.9	20.3	21.6	17.7

As we can discern from the above table, solar radiation in Anogia is higher compared to Tavronitis because the size of the equipment (photovoltaics, batteries, and electrolyzer) required in all three scenarios to achieve the respective goal is much smaller in Anogia compared to Tavronitis. The smaller equipment size also results in lower expenses for its purchase, and therefore, a lower selling price for hydrogen at the end of each year if the installation of photovoltaics is done in Anogia and not in Tavronitis.

Table 5.2 Comparison of results regarding the operation of the battery and electrolyzer.

	Anogia			Tavronitis		
	Scenario 1	Scenario 2	Scenario 3	Scenario 1	Scenario 2	Scenario 3
Battery charging time, %	19.5	27	24.8	31.7	31.2	23.1
Battery discharging time, %	19.5	40.7	36.8	36.7	28.1	40.1
Electrolyzer operating time,%	37.4	60.4	49.1	46.7	35.9	57.9

Table 5.3 Comparison of results regarding the final energy amounts.

	Anogia			Tavronitis		
	Scenario 1	Scenario 2	Scenario 3	Scenario 1	Scenario 2	Scenario 3
Energy by battery to electrolyzer, kWh	2887.8	42323	596060	6960.2	69083	464020
Energy by RES to battery ,kWh	3124	46074	517950	7440.9	68309	446270
Energy by RES to electrolyzer, kWh	8575.6	72330	550180	4504.2	45542	682320
Lost energy, kWh	0.4	34.4	0	0	0	0

In Anogia, the surplus power from the RES that feeds the electrolyzer, activating it to produce hydrogen, greatly exceeds the power supplied by the battery to the electrolyzer. In contrast, in Tavronitis, the energy provided by the RES for the electrolyzer's activation is lower than what the battery supplies. Additionally, it's worth noting that the RES provides more energy to the battery in Tavronitis compared to Anogia, resulting in less energy consumption in Tavronitis.

Community 2

For community 2 the load demand is depicted in Figure 5.1 and it ranges from 3 kW to 18 kW.

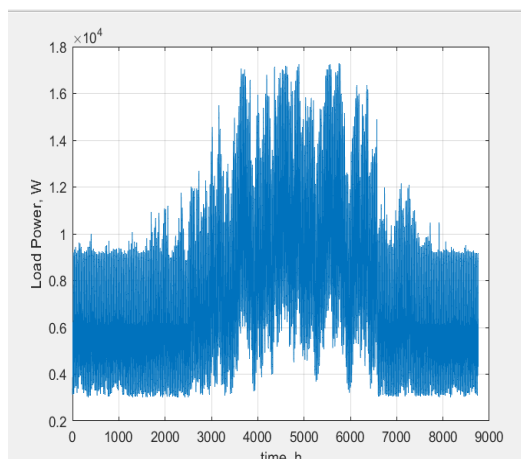


Figure 5.1 Load demand of community 2

Below are the results of the simulation for community 2, which includes one house and hydrogen production. The results are both for the Anogia and the Tavroniti.

Table 5.4 Comparison of results concerning the system.

	Anogia			Tavronitis		
	Scenario 1	Scenario 2	Scenario 3	Scenario 1	Scenario 2	Scenario 3
Size of PV, kW	43.7	153.8	698.8	55.1	132.4	897.2
Size of BAT, Ah	30344.2	6865.5	119660.6	25240.6	21487	89208.1
Size of ELEC, kW	8.5	51.9	838.7	9.2	129.8	586.5
Size of TANK, m ³	20	200	2000	20	200	2000
Investment cost, €	114710	321860	1943700	130500	343160	2124200
Hydrogen selling price, €	60.8	22.8	16.7	81.4	27.8	16.7

As we can discern from the above table, solar radiation in Anogia is higher compared to Tavronitis because the size of the equipment (photovoltaics, batteries, and electrolyzer) required in all three scenarios to achieve the respective goal is much smaller in Anogia compared to Tavronitis. The smaller equipment size also results in lower expenses for its purchase, and therefore, a lower selling price for hydrogen at the end of each year if the installation of photovoltaics is done in Anogia and not in Tavronitis.

Table 5.5 Comparison of results regarding the operation of the battery and electrolyzer.

	Anogia			Tavronitis		
	Scenario 1	Scenario 2	Scenario 3	Scenario 1	Scenario 2	Scenario 3
Battery charging time, %	25.5	14.4	15.2	26.1	16.1	14.3
Battery discharging time, %	69.9	63.2	65.5	69.2	67.7	65.3
Electrolyzer operating time,%	17.5	30.9	39.1	16.6	21.9	39.3

Table 5.6 Comparison of results regarding the final energy amounts.

	Anogia			Tavronitis		
	Scenario 1	Scenario 2	Scenario 3	Scenario 1	Scenario 2	Scenario 3
Energy by battery to electrolyzer, kWh	98817	1890100	157710000	111840	7970600	107500000
Energy by RES to battery ,kWh	32967000	36372000	143850000	33161000	41207000	112990000
Energy by RES to electrolyzer, kWh	11451000	114390000	988470000	11423000	106200000	1059800000
Lost energy, kWh	1610700	74643000	0	1879500	0	0

In Anogia, the surplus power from the RES that feeds the electrolyzer, activating it to produce hydrogen, greatly exceeds the power supplied by the battery to the electrolyzer, as well as in Tavronitis, except the third Scenario, in which the energy provided by the RES for the electrolyzer's activation is lower than what the battery supplies. Additionally, it's worth noting that the RES provides mainly more energy to the battery in Anogia compared to Tavronitis, resulting in less energy consumption in Anogia.

The simulation results revealed that both regions of Crete are suitable for installing photovoltaic systems aimed at covering specific demand loads, but the region of Anogia has higher solar radiation and lower air temperature than the region of Tavronitis, so it is more cost efficient to install photovoltaic systems in Anogia. These regions allow photovoltaics to actively contribute to energy generation, especially during the summer months when solar radiation is high. The total power generated from Renewable Energy Sources (RES) shows a significant surplus throughout the year, enabling the electrolyzer to produce hydrogen.

At the same time, the targets set by the European Union and the European Parliament are encouraging, aiming to reduce greenhouse gas emissions by 55% by 2030 compared to the levels of 1990. This commitment is driving the transition towards renewable energy sources. Today, Renewable Energy Sources (RES) are taken into account in the official energy planning of developed countries, although they still represent a small percentage of the energy production. However, with further utilization, the electricity generated from these sources is expected to decarbonize a significant portion of energy consumption in the EU by 2050.

Hydrogen serves as an energy transporter and storage medium and has numerous potential applications in industries, transportation, energy, and buildings. The most significant aspect is its non-CO₂ emitting nature, leading to virtually zero atmospheric pollution during usage. Despite hydrogen's abundance in nature in practically inexhaustible quantities, it is bound in the majority of cases within water molecules, consisting of two hydrogen atoms and one oxygen atom. Consequently, while water is plentiful on our planet, breaking down the molecule requires energy. Hydrogen, as an energy source, appears as a promising technology, and due to all these reasons, it becomes essential in supporting the EU's commitment to achieving a carbon-neutral balance by 2050.

Literature

English

[1] Hannah Ritchie and Max Roser, 'Energy production and Consumption' and 'CO₂ emissions', Our World in Data, n.d. Accessed Mai 2023

<https://ourworldindata.org/energy-production-consumption#how-is-global-energy-consumption-changing-year-to-year>

<https://ourworldindata.org/co2-emissions>

[2] Djamila Ghribi , Abdellah Khelifa , Said Diaf and Maïouf Belhamel. 2013. "Study of the hydrogen production system by using PV solar energy and PEM electrolyser in Algeria"

<https://doi.org/10.1016/j.ijhydene.2012.09.175>

[3] Balat, Mustafa. 2005. "Usage of Energy Sources and Environmental Problems." Energy Exploration and Exploitation 23 (2): 141–68.

<https://doi.org/10.1260/0144598054530011>.

[4] Veziroğlu, T. Nejat, and Sümer Şahin. 2008. "21st Century's Energy: Hydrogen Energy System." Energy Conversion and Management 49 (7): 1820–31.

<https://doi.org/10.1016/j.enconman.2007.08.015>.

[5] Iberdrola. Green hydrogen: an alternative that reduces emissions and cares for our planet.

<https://www.iberdrola.com/sustainability/green-hydrogen>

[6] EUROPEAN COMMISSION

<https://eur-lex.europa.eu/legal-content/EN/TXT/PDF/?uri=CELEX:52020DC0301>

Greek

[7] Δημήτρης Ιψάκης. 2011. “Σχεδιασμός βέλτιστης λειτουργίας ενεργειακών συστημάτων με χρήση ανανεώσιμων και εναλλακτικών πηγών”. Διδακτορική Διατριβή. Αριστοτέλειο Πανεπιστήμιο Θεσσαλονίκης.

In English:

Dimitris Ipsakis. 2011. “Design of optimal operation of energy systems using renewable and alternative sources”. PhD Thesis. Aristotle University of Thessaloniki.
<http://hdl.handle.net/10442/hedi/24029>

[8] Ντζαχρήστου Χριστίνα. 2022. “Σχεδιασμός και Βελτιστοποίηση Υβριδικού Συστήματος Παραγωγής Πράσινου Υδρογόνου”. Διπλωματική εργασία. Πολυτεχνείο Κρήτης.

In English:

Ntzachristou Christina. 2022. “Design and Optimization of a Hybrid Green Hydrogen Production System”. Diploma Thesis. Technical University of Crete.
<http://purl.tuc.gr/dl/dias/7C63D815-7D30-439B-B489-3C728891760B>

[9] Αναστασίου Νικόλαος και Δόγρανλης Κωνσταντίνος Ραφαήλ. 2021. “Υδρογόνο: Προοπτική για ένα ουδέτερο ενεργειακά περιβάλλον”. Διπλωματική εργασία. Αριστοτέλειο Πανεπιστήμιο Θεσσαλονίκης.

In English:

Anastasiou Nikolaos and Dogranlis Konstantinos Rafail. 2021. “Hydrogen: Prospects for an energy-neutral environment”. Diploma Thesis. Aristotle University of Thessaloniki.
<http://ikee.lib.auth.gr/record/334972/files>

[10] Παπαδημητρίου Χρήστος. 2008. “ΑΝΑΠΤΥΞΗ ΑΛΓΟΡΙΘΜΟΥ ΔΙΑΧΕΙΡΙΣΗΣ ΛΕΙΤΟΥΡΓΙΑΣ ΟΛΟΚΛΗΡΩΜΕΝΟΥ ΣΥΣΤΗΜΑΤΟΣ ΠΑΡΑΓΩΓΗΣ ΗΛΕΚΤΡΙΚΗΣ ΕΝΕΡΓΕΙΑΣ ΑΠΟ ΑΝΑΝΕΩΣΙΜΕΣ ΠΗΓΕΣ ΕΝΕΡΓΕΙΑΣ ΜΕ ΤΑΥΤΟΧΡΟΝΗ ΠΑΡΑΓΩΓΗ, ΑΠΟΘΗΚΕΥΣΗ ΚΑΙ ΧΡΗΣΗ ΥΔΡΟΓΟΝΟΥ”. Διπλωματική εργασία. Αριστοτέλειο Πανεπιστήμιο Θεσσαλονίκης.

In English:

Papadimitriou Christos. 2008. “DEVELOPMENT OF AN ALGORITHM TO MANAGE THE OPERATION OF AN INTEGRATED SYSTEM FOR THE PRODUCTION OF ELECTRICITY FROM RENEWABLE ENERGY SOURCES WITH SIMULTANEOUS PRODUCTION, STORAGE, AND USE OF HYDROGEN”. Diploma Thesis. Aristotle University of Thessaloniki.
http://users.auth.gr/~seferlis/diploma_el_files/2008_Papadimitriou_Christos.pdf

[11] Καρανάσιου Α. Αικατερίνη. 2013. “Μοντελοποίηση συσσωρευτών σε δίκτυα με μετατροπείς ηλεκτρονικών ισχύος”. Διπλωματική Εργασία. Αριστοτέλειο πανεπιστήμιο Θεσσαλονίκης.

In English:

Karanasiou A. Aikaterini. 2013. “Modelling of accumulators in networks with power electronic converters”. Diploma Thesis. Aristotle University of Thessaloniki.

<http://ikee.lib.auth.gr/record/291694/files>